Final accepted copy of
Bakker, M. Costa, A., Silva, T. A. Stutenbecker, L., Girarclos, S., Loizeau, J.-L., Molnar, P., Schlunegger, F. and Lane, S. N., 2018. Combined flow abstraction and climate change impacts on an aggrading Alpine river. Water Resources Research, 54, 223-42
A fully typeset version is available at https://rdcu.be/bBgdF

Combined flow abstraction and climate change impacts on an aggrading Alpine river

M. Bakker[1], A. Costa[2], T.A. Silva[3,4], L. Stutenbecker[5], S. Girardclos[4,6], J.-L. Loizeau[3,4], P. Molnar[2], F. Schlunegger[5] and S.N. Lane[1]

[1] Institute of Earth Surface Dynamics, University of Lausanne, Switzerland.

[2] Institute of Environmental Engineering, ETH Zürich, Switzerland.

[3] Department F.-A. Forel for Environmental and Aquatic Sciences, University of Geneva, Switzerland.

[4] Institute for Environmental Sciences, University of Geneva, Geneva, Switzerland.

[5] Institute of Geological Sciences, University of Bern, Switzerland.

[6] Department of Earth Sciences, University of Geneva, Geneva, Switzerland.

Corresponding author: Maarten Bakker (maarten.bakker@unil.ch)

Key Points:

- Hydropower related flow abstraction may drastically reduce sediment transport capacity, but only to rates that are of similar magnitude as sediment supply.
- This causes downstream river bed aggradation and morphodynamics to be very sensitive to external forcing mechanisms related to flow management or climate change.
- Climate-driven sediment supply may propagate through Alpine streams despite large-scale flow abstraction.

Abstract

Recent climatic warming and associated glacial retreat may have a large impact on sediment release and transfer in Alpine river basins. Concurrently, the sediment transport capacity of many European Alpine streams is affected by hydropower exploitation, notably where flow is abstracted but the sediment supply downstream is maintained. Here, we investigate the combined effects of climate change and flow abstraction on morphodynamics and sediment transfer in the Borgne River, Switzerland. From photogrammetrically derived historical Digital Elevation Models (DEMs) we find considerable net aggradation of the braided river bed (up to 5 meters) since the onset of flow abstraction in 1963. Reaches responded through bed level steepening which was strongest in the upper most reach. Widespread aggradation however did not commence until the onset of glacier retreat in the late 1980s and the dry and warm years of the early 1990s. Upstream flow intake data shows that this aggradation coincided with an increase in sediment supply, although aggradation accounts for no more than 25% of supplied material. The remainder was transferred through the studied reaches. Estimations of bed load transport capacity indicate that flow abstraction reduces transport capacity by 1-2 orders of magnitude. Whilst residual transport rates vary with morphological evolution, they are in the same order of magnitude as the sediment supply rates, which is why significant transport remains. However, the reduction in transport capacity makes the system more sensitive to short-term (annual) changes in climate-driven hydrological variability and climate-induced changes in intake management and sediment delivery rates.

1 Introduction

Many European Alpine glaciated basins are heavily impacted by hydropower exploitation. Besides classical flow impoundment, flow abstraction for within or between valley transfer is a common practice to cumulate hydroelectric capacity from multiple (adjacent) basins (Margot et al., 1992). Whereas reservoir dams tend to trap sediment behind them, leading to downstream sediment starvation (Petts & Gurnell, 2005; Williams & Wolman, 1984), run-of-the-river (e.g. Csiki & Rhoads 2014) and flow abstraction schemes effectively allow sediment to pass through the river. Although the latter may be of primary relevance in Alpine regions, there are relatively few studies of their impacts upon sediment transport (e.g. Fergus, 1997; Raymond Pralong et al., 2015; Turowski & Rickenmann, 2009; Wold & Østrem, 1979) and very few studies of their downstream morphological impacts (e.g. Gurnell 1983). As sediment production and delivery rates tend to be high in mountain environments (Hinderer et al., 2013), the volume of sediment that is trapped at flow intakes may be significant such that frequent purges are required to release sediment down the river (e.g. Bezinge et al., 1989). However, due to the reduction in total flow and with it transport capacity, the rate of downstream sediment transfer should be reduced and consequently lead to temporary or even permanent sediment accumulation (Gabbud & Lane, 2016; Lane et al., 2014). River bed aggradation in the affected Alpine streams may have profound impacts on riparian ecosystems (Gabbud & Lane, 2016; Petts & Bickerton, 1994) and infrastructure through increased risk of flooding (Lane et al., 2007), lateral channel instability and bank erosion (Church, 2006; Wheaton et al., 2013), and damage due to high sediment loads (Badoux et al., 2014; Hilker et al., 2009). On a larger scale, the sediment delivery to main rivers and deltas may be affected (Costa et al., 2017).

The direct impacts of human activity on river flow and hence sediment transport that arise from hydropower exploitation may be amplified by the indirect effects of human impacts that are manifest through climate change. Since the little Ice Age, large accumulations of unconsolidated sediment, derived from weathering and glacial erosion, have become available for transport (e.g. Haeberli & Beniston, 1998; Stoffel & Huggel, 2012). In the traditional model of paraglacial response (Ballantyne, 2002; Church & Ryder, 1972), the onset of glacial recession leads to high initial rates of geomorphic activity followed by a process of relaxation as a series of negative feedbacks create progressively greater levels of landscape stability. A critical question then follows as to what happens in such Alpine basins subject to accelerated climatic warming (e.g. Beniston et al., 1994; Gobiet et al., 2014) and associated glacial retreat which has been observed during the last decades (Haeberli & Beniston, 1998; Haeberli et al., 2007; Heckmann et al., 2016; Paul et al., 2004) and is projected in the future. There have been few studies that address the transient state of these environments (Haeberli & Beniston, 1998; Lane et al., 2017). An increase in fluvial sediment supply may be the direct result of greater access to freshly exposed subglacial sediment (Lane et al., 2017; Warburton, 1990) as well as the effects of increased sediment transport capacity associated with more rapid ice melt (Raymond Pralong et al., 2015). Indirectly, sediment is also derived from hillslope erosion due to glacial debuttressing (Curry et al., 2006; Holm et al., 2004; Norton et al., 2010) and general permafrost degradation (Fischer et al., 2013; Gruber & Haeberli, 2007; Stoffel & Huggel, 2012). The actual system response to increased sediment supply is however complex (Harbor & Warburton, 1993), because the sediment flux through the landscape depends on the interaction between landforms and processes, including feedbacks and conditioned through the connectivity amongst them (Cossart & Fort, 2008; Geilhausen et al., 2013; Lane et al., 2017).

Thus, both flow abstraction and climate change are likely to have important consequences for sediment transfer and river morphodynamics in Alpine streams and their ecosystems. Yet, despite recognition of the need to factor sediment into water resource management (Wohl et al., 2015), there are very few studies of river response to human forcing of streamflow in combination with indirect human forcing of climate. This can be related to difficulties in quantifying the acting geomorphic processes, typically topographic change and bedload transport, on the relevant annual to decadal timescale, and the complexity and interaction of the processes involved. In this context, we aim to investigate the extent to which flow abstraction slows down the effects of rapid climate warming upon stream flow and sediment supply from propagating downstream through Alpine streams.

We focus on the Arolla Valley, Switzerland, which has long term discharge records from flow intakes from which it is possible to reconstruct a unique record of reliable coarse sediment supply rates (e.g. Bezinge et al., 1989). Lane et al. (2017) and Micheletti & Lane (2016) used these to investigate the impact of climate change on sediment production and export from basins upstream of flow intakes. In this study we use the same approach and, in addition, use archival photogrammetry to assess the impact of flow abstraction on the river bed evolution and sediment transfer downstream of hydropower intakes. The objectives of this paper are: (1) to quantify the evolution of river morphology and sediment transfer at the decadal time-scale; and (2) to assess the relative and combined impacts of climate change and hydropower exploitation on this evolution.

2 Study area

The Grande Dixence hydropower scheme is located in the Pennine Alps of south-west Switzerland. It produces approximately 2 billion kWh of power per year and accounts for 20% of Switzerland's energy storage capacity. Constructed in the late 1950s, it abstracts water from the headwaters of two Upper Rhône tributaries, the Vispa and Borgne, via 75 flow intakes (Park, 1980). The water is transferred through a network of 100 km of tunnels and 4 pumping stations to the Lac de Dix (Figure 1a), a retaining reservoir in the adjacent Dixence catchment (Tanchev, 2014). From there the water is supplied to 4 hydropower stations in the Rhône valley (Bezinge et al., 1989; Gurnell, 1983).

In this work we focus on the upstream part of the Borgne d'Arolla (Figure 1a), where flow has been abstracted since 1963 when the Lower Bertol (LB) intake (Figure 1b) and Arolla pumping station became operational. It is largely fed by the Bas Glacier d'Arolla (also known as the Glacier de Mont Collon) but indirectly also receives water and sediment from regulated catchments upstream through purges from three intakes. These are the Upper Bertol (Micheletti & Lane, 2016) and Vuibé tributary catchments, and most notably the Haut Glacier d'Arolla (HGdA) catchment (which has a surface area nearly 1.5 times that of the Lower Bertol). Sediment export from the latter catchment, investigated by Lane et al. (2017), enters the LB catchment on the flank of the retreating tongue of the Bas Glacier (Figure 1b).

Under normal flow conditions, all water is abstracted by the flow intakes. Downstream, the flow gradually increases due to unregulated tributaries, lateral drainage and ground water emergence. During a purge from the LB intake, sediment is evacuated from a trap and is transferred downstream into a series of four braided river reaches, A through D (Figure 1b, 1c), which are separated by narrow, incised, semi-alluvial reaches (only reach C and D are more or less directly connected), and so are considered to be transport zones. A major tributary that is also subject to flow abstraction is the Tsijiore Nouve (TN) which has a relatively high sediment yield (as compared to LB; Gurnell et al., 1988) and enters the Borgne d'Arolla between reaches A and B (Figure 1c). The studied braided reaches were established before the onset of hydropower activities (SwissTopo, 1946; Supporting Information S1, reach A, 1959), their presence associated with local valley widenings and reduced stream gradients upstream of tributary alluvial fans (Figure 1b, 1c). Further downstream, though not directly part of study area, the Borgne alternates between steep, e.g. between Reach D and Les Haudères, and channelized sections, e.g. between Les Haudères and Evolène; Figure 1a), the latter which have a Post-Glacial history of braiding terraces (Small, 1973).

3 Methods

3.1 Overview

In this study we draw upon two main sources of data to analyze the evolution of river bed level and sediment supply. First, we apply an archival photogrammetric method developed by Bakker & Lane (2017) to determine topographic and morphologic change of 4 braided river reaches since 1959, just before the onset of hydropower exploitation. Second, a record of the flow intake, just upstream of the reaches is used to quantify discharge, both the total 'natural' discharge that would have occurred without hydropower exploitation and the residual 'purge' discharge associated with intake flushing. This also allows us to determine sediment supply to the studied river reaches as a function of the number and type of purges associated with emptying the sediment traps. From the determined topographic change and sediment supply we calculate sediment transfer through the system. Finally, we analyze the forcing mechanisms that have contributed to the system evolution: (1) we quantify the impact of flow abstraction and regulation on transport capacity using a bed load equation; and (2) we compare climatic variability in seasonal temperature and precipitation to the variation in upstream sediment delivery.

3.2 Morphologic change based on photogrammetry

3.2.1 SfM archival photogrammetry

Topographic data is acquired using Structure from Motion (SfM) based photogrammetric methods which are described in full in Bakker & Lane (2017) and briefly summarized here. Scanned historical images are provided by the Federal Office of Topography (SwissTopo) for the period 1959-2005, with intervals of 4-12 years. Photographs from a specially commissioned low elevation flight in 2014 are used to extend the record. Pix4D, a commercially-available software package, is used to perform photogrammetric reconstruction based on 15-25 ground control points and abundant tie-points generated using computer vision algorithms. This results in a bundle adjustment quality (i.e. reprojection error and control point RMSE), similar to values derived using classical techniques (Bakker & Lane, 2017). An overview of the image and bundle adjustment data is given in Table 1. The resulting densified point clouds are analyzed for potential systematic errors, resulting from random error in the bundle adjustments (Lane et al., 2004), and these errors are minimized through point cloud registration. Stable zones from an additional dataset, a 2 m resolution airborne laser scan survey for the year 2010 (ALTI3D data provided by SwissTopo), are used as a reference. The referenced point clouds are used to generate collocated 1 m resolution Digital Elevation Model (DEM) grids (Bakker & Lane, 2017).

In addition to providing DEMs, the photogrammetric analysis also produces orthoimages (provided in Supporting Information S1) with a ground resolution of 0.09-0.5 m (Table 1). These were used for morphological interpretation where we assess: sedimentation width defined as the active channel width plus overbank deposits, river morphology and channel configuration, riparian vegetation, human impact and surface grain size.

3.2.2 Topographic change

Local error in the DEMs is assessed based on orthoimage texture which was shown to have a strong impact on the ability of SfM methods to extract and match 3D tie-points (Bakker & Lane, 2017). We quantify error using an entropy filter (with a 9x9 cell running window) and inversely scale the obtained values to 0.5-2 times the theoretical precision which is estimated from the ground resolution. See Supporting Information S2 for further details. DEMs of difference (DoDs) are generated to quantify net topographic change, using basic error propagation (Brasington et al., 2003; Lane et al., 2004) and probabilistic thresholding (Lane et al., 2003; Wheaton et al., 2010). In this setting, the temporal resolution of the images is insufficient to assess morphological change using spatial coherence (Wheaton et al., 2013; Wheaton et al., 2010), resulting in multiple non-coherent changes. We did add two basic constraints to filter local outliers from the DoDs: (1) a limit for maximum absolute change in elevation between consecutive DoDs (4 m) and; (2) a limit for maximum opposite changes between consecutive DoDs (±1.5 m), i.e. 1.5 m of erosion may be followed by 1.5 m sedimentation (or vice versa). In the latter case we average the consecutive change values as it was likely that there is an error in the common DEM. The resulting DoDs are clipped to the maximum sedimentation width, excluding areas where (temporary) sediment mining and construction took place. We then use the DoDs to determine net volume changes and mean elevational changes for the consecutive periods along the river channel, based on 90% confidence limits (Lane et al., 2003). This provides us with a record of the decadal river bed evolution and give us some insight (snapshots) in the shorter term (annual) morphodynamics.

3.2.3 Channel gradient and sediment grain size

We determine channel gradient and sediment grain size both to quantify their (relative) downstream trends and as input for further bed load transport capacity calculations. The mean gradient of the river channel is determined from the 2014 DEM (Figure 2). Local field measurements of surface sediment grain size were performed using the Wolman (1954) count, grid-by-number approach (Supporting Information S3). These values are spatially extrapolated through two-dimensional semivariogram analysis of the 9 cm resolution 2014 orthoimage; for details on this method see Carbonneau et al. (2004). We use a 25x25 cell running window (2.25 x 2.25 m) for which we quantify the semivariogram range distance and sill value. Both measured D_{50} (R^2= 0.77, $p<0.001$) and D_{84} (R^2= 0.82, $p<0.001$) show statistically significant relations with the bilinearly interpolated sill value (Supporting Information S3), despite the use of a relatively coarse image resolution. Because channel location and grain size vary in time, we derive a value for the regularly inundated section of the channel as the 20th percentile of the sill values within the cross section (Figure 2). These values are in general agreement with a D_{50} of 18-35 mm found by Warburton (1992) in the proglacial zone, upstream from the intake.

3.3 Discharge and sediment supply

3.3.1 Flow intake record and purge identification

The main flow intake that we consider in this paper is the Lower Bertol (LB), for which we describe: (1) how the system functions and is operated; (2) how we used this to acquire up- and downstream discharge and sediment delivery. In addition we derive data for the TN intake, which functions in a similar way to LB and is hence treated using the same method (see Supporting Information S5), and also use data of the HGdA intake from Lane et al. (2017).

The LB intake comprises two sediment traps (Bezinge et al., 1989; Gurnell et al., 1988): (1) a gravel and coarser material trap, which is purged using manual controls; and (2) a subsequent sand trap which is purged automatically. Flow enters the intake via the gravel trap, where the coarse bed load (gravel-boulders) is caught, and the water passes through a grill into the underground sand trap designed to allow sediment to settle out of suspension. The remaining flow, which has only wash load, passes over a broad crested weir and enters the hydropower tunnel system. The amount of water abstracted is measured using a stage recorder at the broad crested weir in the intake and logged for regulatory reasons. A 15-minute interval time series for the period 1977-2014 is provided by Grande Dixence SA for the LB and TN intakes. During purges, the gates of one of either of the sediment traps are opened and water is allowed to flow down the river, flushing sediment with it (Figure 1 photo insert). This causes a rapid drop in water level at the weir and the intake of flow is temporarily stopped for the duration of the purge (Figure 3a).

To obtain the total upstream discharge, we need to account for the periods of interrupted flow measurement during purges. As a first means of purge identification, we determined all instances where the discharge drops to zero, i.e. a 100% reduction, in a single time step. Where the data is averaged on a 15-minute basis, the intake time-series may however not always reach zero, depending on the timing and duration of the purge, and therefore anomalously large discharge drawdowns need to be identified. We distinguish these by considering the frequency distribution of the relative changes in discharge per 15-minute time step (Figure 3b). We note that under normal flow conditions, the occurrence of frequent fluctuations is typically described by a logarithmic distribution. If we extrapolate this, large drawdowns occur very rarely (dotted line). However, in practice, due to flow regulation, large drawdowns occur frequently due to the onset of purges. Where there is a transition in the distributions of the normal and purged flow we find a break in slope (Figure 3b), which we use to identify purges. The purges are visually verified, where the HGdA discharge record (Lane et al., 2017) is used as a reference to aid this process. In addition, we assess purges based on a minimum required flow volume to empty the sediment trap (600 m^3; Figure 5).

Once the purges are identified, we apply linear interpolation to the intake time series over the duration of each purge to estimate both the purge discharge down the river and the upstream total discharge that arrives at the intake, the sum of the intake and purge discharge (Figure 3a). When LB purges coincide with those from upstream intakes, notably the HGdA, the discharge interpolation may lead to an underestimate. This is a common practice during night-time purges which were introduced in 2008 for safety reasons (to reduce the frequency of dangerously high flows during the day time) and to enhance sediment throughput. Occasionally, this is also a necessary practice when, during high flow events, the flow intake and transfer system is near or at its maximum capacity and flow abstraction must be stopped (Park, 1980). This results in longer duration, high flows in the river downstream of the intake. From the HGdA and LB time series we determine the wave propagation time between the intakes as approximately 1 hour (± 15 min) by considering those purges from the HGdA that can be distinguished in the LB flow intake data (i.e. when the latter is not purging). For these events we perform linear regression analysis to determine the relation between the HG interpolated purge discharge and LB intake discharge, taking into consideration the required propagation time (Figure 4). Vice-versa, we also determine the relation between the measured HGdA intake discharge and measured LB interpolated purge discharge. This gives a lower slope due to the absence of the contribution of the HGdA purging (Figure 4). Based on the difference between these regression slopes over the period 1988-2013, we can account for an increase in the LB discharge equal to about 35% of the discharge that was released at the HGdA during purging, and we add this to the LB purges to get a discharge estimate of the coinciding purges. We use this in the evaluation of the impact of flow intake management.

3.3.2 Sediment supply from purge frequency

Because of the nature of the operating conditions, the intake data can also be used to infer the supply of bed load and suspended load to the intake and sediment delivery to the downstream reach. For the period 1977 to 1987 we use sediment load quantified by Bezinge et al. (1989), based on purge frequency and the dimensions of the LB sediment traps. They estimated the effective volume of purged sediment to be 150 m^3 for the gravel trap and 8 m^3 for the sand trap based on turbidity measurements and sediment height surveys in the gravel trap. Besides loads, it is also possible to obtain an indication of sediment grain size through distinguishing gravel and sand trap purges.

For the period 1988-2014, we use the estimated volume of water that is released per purge to distinguish the type of purge. We base this on a cumulative frequency analysis as shown in Figure 5. On the basis of the sand trap dimensions and a typical purge duration of less than 20 minutes, we estimate that up to 1500 m^3 of water is required to evacuate the sand, which may be distinguished in the low occurrence frequency around this value (Figure 5). Purges of the gravel trap are longer, often more than 30 minutes, and are characterized by higher water volumes required to remove much larger amounts of sediment with greater resistance to motion. There is also greater variation in the water volume released due to their manual operation. Here, we distinguish night-time (just before midnight) purges which occur since 2008 when the gravel trap is more than half full. For these purges we assign 80% of the full intake capacity with an error of ±20%, following Lane et al. (2017). Lastly, we identify high water volumes, larger than 17000 m^3, which are associated with (near) system surcharge events where flow cannot be abstracted, typically for a few hours, due to capacity limitations of the hydropower system. The sediment load is not easy to quantify where it doesn't accumulate to a known (sediment trap) volume but passes directly through. Based on the flow volume and typical duration (hours), we assign a sediment volume of 4±1 times the gravel trap capacity as an estimate of the sediment supply. To verify the cumulative frequency analysis we used purges identified from a minute-based time-series for 2015, which shows a similar volume frequency distribution, and for which a number of purges were observed and identified in the field. The same procedure was followed to establish sediment delivery for the TN intake (Supporting Information S5).

The process of purge (type) identification and the calculation of sediment volumes contains a number of assumptions and uncertainties. We therefore identified a range in sediment supply where lower and upper limits are defined based on flow reduction for purge identification, 100% flow reduction and large drawdowns respectively, and sediment supply using ± estimates. We would however like to emphasize that the obtained time series of sediment supply may be considered to be fairly unique with regard to its accuracy, given the difficulty of measuring bed load transport rates directly, and its timespan which covers decades (this was already recognized in the late 1980s by Bezinge et al., 1989; Gurnell et al., 1988).

3.4 Sediment budget and sediment transfer

We evaluate net sediment storage and transfer in the river reaches through applying a sediment budget approach (Warburton, 1990), which forms the basis to evaluate the system response to climate and human impacts (e.g. Harbor & Warburton 1993). Although this approach may underestimate sediment transfer (Lane et al., 1994; Lindsay & Ashmore, 2002), in this case the aggradational nature of the braided reaches and particularly the continuous record of sediment delivery from the LB intake, allow us to quantify sediment transfer more confidently. Since 1977, from which date we have sediment supply, the average annual sediment transfer rate is calculated for periods between the available aerial photographs for reach A individually and the combined reaches B, C and D. From the intake sediment supply and the net morphological change in reach A, i.e. the change in sediment storage, we estimate the average sediment transfer rate through the reach following the Exner equation (after Ashmore & Church, 1998), assuming constant packing density (that is the packing density in the sediment traps is equal to that of the aggraded river bed). We do not account for sediment input from local bank erosion or sediment lost to gravel mining and river works, where they are difficult to distinguish and the latter largely involves the reworking of sediment within the reaches (rather than its removal) due to legislative constraints. Sediment that is transferred out of reach A is transported through a narrow, incised river section that stores negligible sediment and forms the upstream supply to the combined reaches B, C and D. Here, we correct for the possible sediment transfer from the TN intake, which ranges between 0 and 100% of the supplied sediment. We do this because we seek to compare the sediment transfer efficiency of sediment that originates from the LB intake between reach A on one hand and reaches B, C and D on the other hand, and not to analyse the transfer of sediment from the TN intake itself or the total sediment flux. Lastly, we note that wash load, though potentially significant in amount, is not considered in this context due to its absence in the supply record and its subordinate relevance in the downstream morphodynamics.

3.5 Sediment transport capacity and Supply-Capacity Ratio (SCR)

Bed load transport capacity is modelled using the same approach as Lane et al. (2017) and following (Nitsche et al., 2011), where we: (1) reduce the energy gradient due to flow resistance associated with river-bed macro-roughness based on Ferguson (2007); (2) determine transport capacity using the shear-stress based bed load equation of Rickenmann (1991) that was shown to perform well in Swiss mountain streams (Nitsche et al., 2011); and (3) account for transport of finer sub-surface material during armour layer breakup (Hunziker & Jäggi, 2002), relevant in this setting (Warburton, 1992). See Supporting Information S4 for details. We quantify bed load transport capacity using discharges measured at the LB intake, and a cross section 750 m downstream of the intake (CS in Figure 1a). This location is chosen to be directly downstream of a narrow (partly channelized) and steep section, just beyond a knick-point in slope (S) and grain size (D_{50}, D_{84}), as shown in Figure 2. Here, the channel is at its widest and the largest aggradation is expected (Lane et al., 2014). Flow attenuation between the intake and this location is expected to be minimal. As the morphology is temporally (and spatially) variable, we calculate a range in transport capacity based on the cross sections from the DEMs in the period 1988-2014 (Supporting Information S6). To compare the results with purged sediment volumes, we determine the volumetric transport capacity (V) based on the gravel trap packing density s=1300 kgm^{-3}, as established by Bezinge et al. (1989).

The modelling approach provides bed load transport capacity estimates for the period 1977-2014. The results are analysed using a Supply-Capacity Ratio (SCR) where the annual sediment supply that passes the intake is divided by cumulative annual transport capacity, so as to give a relative measure of the variation in sediment surplus that is supplied to the river (Lane et al., 2017). We use this measure gain insight in the evolution of the sediment budget and to evaluate the human impact through comparison with the transport capacity that would have resulted in the absence of flow abstraction.

3.6 Climate change

Widespread temperature increase has been observed in the European Alps (Beniston et al., 1994; Gobiet et al. 2014), being more pronounced at higher elevations (Giorgi et al., 1997). The increase has been particularly strong since the 1980s (Costa et al., 2017) and is projected to continue into the future (Ceppi et al., 2012). In addition to the mean temperature increase, the variability also appears to increase, with more frequently occurring heatwaves (Schar et al., 2004). Precipitation trends are more regional, although here too an increase in variability is expected, associated with enhanced summer convective rainfall (Giorgi et al., 2016).

Such trends, particularly the increase in the 1980s, can also be distinguished in spatially interpolated, daily temperature and precipitation data (MeteoSwiss, 2016a,b) for the Bas Glacier catchment (Figure 6), based on Frei (2014); see also Costa et al. (2017). We aggregated this data to month-based periods that reflect seasonal changes in hydrology and runoff: summer (July – September) and winter/spring (January – May), which we refer to as 'winter' hereafter. Note how these differ to annual averages on a year-to-year basis (Figure 6). This data has the necessary uncertainties for local application, mainly systematic error in absolute values and in the case of precipitation variable error related to underestimation during strong wind (particularly in the case of snow) and high intensity precipitation (MeteoSwiss, 2016b). These however only have a limited effect on our forcing analysis, where we only consider relative changes over a long period of time where temporal weather variability may be expected to average out. Linear regression techniques were used to determine the correlation of summer temperature and winter precipitation on one hand with total annual sediment delivery and water yield at the LB intake on the other hand. Lastly, we determined the covariation of temperature and precipitation in order to assess their individual or combined forcing of sediment supply.

4 Results

4.1 Evolution of river bed aggradation and sediment transfer

4.1.1 Morphological evolution river bed

Over the course of the investigated period, from 1959 to 2014, large scale river bed aggradation took place (Figure 7). Sedimentation is widespread and prominent in all reaches, while net erosion is limited to banks in the upper parts of reaches A and particularly B. The largest increase in bed level, up to 5 m, took place near the upstream end of reach A where the channel widens and the gradient decreases (Figure 2). Not coincidentally, this is also a site of sediment extraction previously used for the construction of hydropower infrastructure (see also 1959 orthoimage of reach A in Supporting Information S1). To aid sediment throughput here, a straight channel was constructed on the right bank in 2012, clearly present as a thin zone of erosion in Figure 7. Reach D also shows extensive aggradation, but less within channel and more in the form of lateral or overbank deposits (Figure 7).

The temporal evolution of the aggradation is shown in Figure 8. Considerable deposition occurred in reach A between 1959 and 1965 (Figure 8a), which can at least be partially related to the onset of flow abstraction in 1963. This was followed by a period with very limited net sediment accumulation which lasted until 1983 in the lower part of reach A and 1988 in the upper part of reach A. A phase of major aggradation, which is also reflected in an increase in both channel width and elevation (Figure 8b, 8c), then took place until 1995. A period of less change is then followed by a second phase of major aggradation between 1999 and 2005. In the last period, until 2014, the long-term trend of persistent aggradation is disrupted by substantial net erosion. Note that over the whole period of net aggradation shorter periods of erosion may have occurred more often, but these cannot be resolved with the temporal resolution of the available topographic data.

Until the early 1980s, reaches B, C and D responded to a lesser degree as compared with reach A, although reach D does show a similar initial response (Figure 8a). In reach B, major aggradation occurred in the period 1983-1988, less so in reaches C and D. This prompted extensive river engineering and straightening in the downstream part of reach B (Figure 8b), while aggradation intensified in reaches C and D in the period 1988-1995. For reaches B through D, volumes of aggradation until 1995 are not much less than in reach A (Figure 8a). Until 2010, there is very limited aggradation and also some local erosion (e.g. between 2005 and 2010). Finally, between 2010 and 2014 sedimentation occurred, particularly in reaches C and D (overbank deposits, Figure 7), which appears to correspond to the erosion and release of sediment from reach A in this period.

Although net aggradation was limited, the river channel morphology changed considerably in the period between 1965 and 1988 as reflected in the sedimentation width (Figure 8b). Initially the channel contracted, adopting a more wandering or meandering character where bars were stabilized and riparian vegetation developed as shown in 1977 (see also orthoimages of reaches A and D in Supporting Information S1). Reach C was actually reduced to a low sinuosity single thread channel. These changes may be associated with the low frequency of channel perturbation and bed reworking following from the short and discontinuous nature of purge flows as compared with normal diurnal discharge cycles. After 1977, the channel expanded again to reach its original extent by 1988, in the process burying and removing most of the vegetation that had developed (see also Lane et al., 2014). This corresponds to the increased aggradation in the 1980s (upper part of reach A and reach B). Large flood events in 1987 (Rey & Dayer, 1990; Warburton & Fenn, 1994;) may have played a significant role in this morphological change. Later changes in sedimentation width (and also grain size; Figure 2) are locally influenced by river works for the protection of the pumping station (reach A), a campsite (reach B) and pastures (reaches C and D) along the river (dikes in Figure 8).

Aggradation since 1988 has led to a development of reach-based gradients in the rise of mean channel elevation. In reach A the bed level shows a sharp increase just downstream of the intake where the channel gradient decreases and the river widens, which then progressively decreases along the reach, effectively steepening the reach (Figure 8c). Together with the downstream fining trend (Figure 2) this illustrates the typical effect of a (maintained) high sediment supply and a significant loss of transport capacity due to flow abstraction and purge attenuation. The lower reaches, which become progressively less steep, mimic this trend although grain size trends are less clear due to TN input, general flow increase and river engineering impacts on channel morphology. These trends in bed level rise suggest that despite the significant (upstream) aggradation, sediment throughput was still sufficient to drive downstream morphological change.

4.1.2 Upstream flow and sediment record

The total annual volume of water arriving at the LB intake is shown in Figure 9a. The intake comprises flows from melt of the Bas Glacier, as well as residual flow (mainly purges) from upstream intakes of which the HGdA has by far the largest contribution. The LB inflow increased gradually in the late 1970s and 1980s, reaching its maximum in the early 1990s. This coincides with a transition from a colder and wetter period in the late 1970s (Micheletti et al., 2015) to a warmer and dryer period in the early 1990s (Figure 6) and a transition from Bas Glacier advance before 1987 (Glaciological reports, 1881-2017) to retreat after 1987. From 1995 onwards the inflow is lower again, but no decreasing trend is observed. Although the Bas Glacier has retreated significantly and lost most of its low altitude ice volume, rising temperature may have increased melt in the higher parts of the basin so sustaining water yield. Since 2003, a rising purge frequency from the HGdA led to an increase in its contribution to the LB flow from approximately 1 to 6% (Figure 9a).

Similar to water yield, the sediment supply to the LB intake shows a steady increase in the 1980s, reaching peak values in the early 1990s (Figure 9b). The latter coincides with the onset of rapid sedimentation in the braided reaches, particularly in reach A (Figure 8a). After a period of lower sediment supply, the rates increased in 2003 and particularly 2011. The evolution of sediment supply is in broad lines similar to that of the HGdA (Lane et al., 2017), which potentially accounts for about 30% of the sediment availability in the Bas Glacier (sub/)pro-glacial area and supply to the LB intake. The TN intake, which enters the Borgne downstream of reach A, shows a purging evolution similar to LB (Supporting Information S5), with the exception that supply rates in the 2000s remain low until 2010 when there is a sharp increase.

The LB purge record may also provide an indication of the sediment composition. We found a relatively low number of sand trap purges when compared to Bezinge et al. (1989), who found that the purge frequency was more or less similar to that of the gravel trap in the period 1977-1989. This could be due to an actual decrease in fine sediment supply, although this cannot be verified due to uncertainties in purge identification related to the small size of the sand trap (and therefore small volume of water required to purge it, which is difficult to detect as a drop in the flow intake series; Figure 3a). Here we would like to emphasize that whilst the number of gravel trap purges fluctuate, the number of sand trap purges remain fairly constant until a systematic increase around 2005 (only 2009 is an exception).

4.1.3 Sediment transfer

Figure 10 shows the evolution of sediment input from the LB intake and the subsequent sediment transfer through reach A and reaches B, C and D since 1977. Although we have no sediment delivery rates from before this period, we can infer that between 1965 and 1977, when net erosion occurred, all incoming sediment (i.e. > 100%) was transferred through reach A. Between 1977 and 1983, the sediment supply rate was low (Figure 9a). This sediment was largely transferred through the reaches (Figure 10b) and there was some net aggradation in the lower part of reach A (Figure 8a). Between 1983 and 1988 there was a substantial increase in sediment input to reach A (Figure 9), but the reaches appear to be able to transfer this increase nearly in its entirety through to the end of reach D. A further increase in supply from the LB intake, (Figure 10a) between 1998 and 1995, led to major river bed aggradation in reach A (Figure 8), and a drop in the relative amount of sediment transfer through the reach (Figure 10b). Reaches B, C and D also show considerable aggradation (Figure 8), but this change could be accounted for by sediment from the TN intake. Between 1995 and 1999, the sediment input to reach A drops markedly (Figure 10a), but the low rate of sediment transfer (Figure 10b) is maintained. The rate of sediment transfer through reach A falls further between 1999 and 2005, which taken with a slight increase in sediment supply results in rapid aggradation (Figure 8a). Given the uncertainty range due to the supply from the TN intake, no significant change could be detected in the transfer of sediment that originates from the LB intake through reaches B, C and D, which remains around 100% during the period 1977 to 2005.

There seems to be a marked change in the system after 2005. Sediment supply at the LB intake rises and reaches a maximum in 2010-2014 since the data begin in 1977 (Figure 10a). Between 2005 and 2010, there is net aggradation in reach A (Figure 8a), with sediment transfer that rises, but remains lower than 100% (Figure 10a). However, reaches B through D degrade during this period (Figure 8b, 10b). The inverse then occurs between 2010 and 2014 when despite very high sediment supply to A (Figure 10a), reach A shows net degradation (Figure 8a) and a high sediment transfer rate (Figure 10b). The latter, in turn, appears to lead to net sedimentation in B through D (Figure 8a) and a sediment transfer rate slightly lower than 100% (Figure 10b).

Over the whole period, more than 75% (76-97%) of the sediment that enters the system is transferred through all reaches. Thus, despite the considerable impacts of flow abstraction and profound morphological changes of the river bed, relatively high rates of sediment transfer downstream are maintained. In addition, it appears that under a system with substantial flow abstraction, relatively small changes in sediment supply can lead to relatively major morphological responses (Figure 8). We develop these points further by assessing bed load transport capacity.

4.2 Forcing of sediment supply and transport capacity

4.2.1 Hydrologic forcing due to flow abstraction

On annual basis, the total fraction of water that is abstracted is in the range of 85% to 99% (Figure 11a). The water that is not abstracted is largely used to evacuate sediment from the intake during purges, resulting in relatively lower amounts of abstraction when there is high sediment supply in the first half of the 1990s and since the mid-2000s (Figure 9b). The capacity of the hydropower intake system to abstract water and at the same time to reduce the residual flow in the river is related to magnitude of the discharge as is shown for different annual exceedance durations in Figure 11a. During high discharges (e.g. flows exceeded less than 1 day per year), the hydropower system is typically operating near its maximum capacity due to abstraction of similarly high discharges from catchments higher up in the system. In this case, the intake of water at the LB intake (but similarly for HGdA and TN) has to be temporarily stopped to prevent the surcharge of the system. A trend emerges, where the effect of flow abstraction becomes less with increasing discharge (Figure 11a). In addition, a temporal trend may be observed since the mid-2000s, where the effect of flow abstraction decreases (for all exceedance durations) to more or less 0 for the highest flows (1 hour per day) since 2010. The latter coincides with a marked increase of (near) system surcharge events (Figure 9b) as the limited capacity of the hydropower system is becoming increasingly insufficient to accommodate the increasing peak discharges from the hydropower catchment, and for periods of some hours, all water delivered to the intake is allowed to pass downstream.

If we consider the Supply-Capacity Ratio (SCR) downstream of the intake under natural conditions (no flow abstraction), values are in the order of 0.02-0.2 (Figure 11b). Thus in this case, sediment supply would be substantially lower than transport capacity throughout the period. From 2005 onwards there is a notable increase in SCR (Figure 11b) which is associated with an increase in sediment load and fairly constant discharge (Figure 9a, 9b). Note that the calculated bed load transport capacity is only indicative as it is artificial to combine the morphology under a flow abstraction regime with a natural flow regime. In reality, SCR values lower than 1 should lead to erosion, channel geometry changes, grain size sorting and stream bed armouring to the point at which the transport capacity is reduced and the SCR tends to one.

Under the actual conditions (with flow abstraction), the SCR is greater than 1 (Figure 11b): the transport capacity of the residual flow is c. 3 times smaller than the supply, which is commensurate with the observed aggradation here (Figure 8a). There is a significant band width associated with these calculations due to uncertainties in sediment supply but more notably due to the effect of temporal changes in morphology (see Supporting Information S6). Morphological change may have led to reinforced transport capacity in periods of relatively low sediment supply, e.g. 1999, or reduced transport capacity in periods of increased sediment supply such as in 2005 (Figure 11b), although we must note that in the same period river engineering also took place. Since the mid-2000s, the SCR values have generally decreased and approached the point at which the increase in purge discharges (Figure 9a) is sufficient to transfer the increasing rate of sediment supply: SCR ≈1 (Figure 11b). This is reinforced by the effect of coordinated purges and occurrence of (near) system surcharge events; note that this effect is negligible (not visible) for the total discharge. Whereas these calculations are an estimation and don't take into account spatial changes in river morphology, they do indicate a tendency towards reduced sedimentation rates and potential erosion in the last few years, particularly for the finer fractions (e.g. sand).

Even with a substantial reduction in transport capacity due to flow abstraction, there remains sufficient flow to transport a significant proportion of sediment through the system, explaining sediment export between 2005 and 2014 in Figure 11b. In addition, the SCR of the natural and purged discharges converge through time, suggesting that the impact of flow abstraction is decreasing. We attribute this change to the changing flow duration (Figure 11a) associated with purge management, in the form of a shift towards coordinated night-time purging, and capacity limitations of the hydropower system, resulting in flow intake limitations and consequent high flow events.

4.2.2 Climate forcing and system response

Sediment supply showed the strongest monthly-based correlation with both average daily summer temperature, in the period July – September, and average daily winter precipitation, in the period January – May. Figure 12a shows that summer temperature directly forces sediment delivery to the intake through ice melt which both releases sediment and affects the magnitude and duration of competent stream flow, that is sediment transport capacity. No relation was found with summer precipitation, however precipitation in the preceding winter is negatively associated with sediment supply; this reflects snow cover persistence which has a buffering effect on the summer ice melt (Figure 12b). Summer temperature and winter precipitation show weak but significant covariation ($p< 0.05$, not shown here) and were therefore reduced to a single principal component which reflects 66% of the common variance. Their combined effect is reflected in the 'climate' principal component (Figure 12c) which reveals a clear and direct, annual response of sediment delivery to climatic conditions.

Based on Figure 12c we identified 4 periods with characteristic sediment delivery due to climate forcing and system response. As a reference we used the linear correlation for the period 1977-1990 ($R^2 = 0.54$, $p < 0.002$), which seems to reflect the ice melt and sediment transfer reasonably well. In this period gradual climatic change (Figure 6) led to a steady increase in sediment delivery (Figure 9b). The particularly warm and dry 1991 marks the beginning of a few years with relatively high sediment delivery rates which may be related to the close-proximity and retreat of the Bas Glacier, with retreat starting not much earlier (since 1987). Following the particularly wet 1995 and cold 1996, sediment delivery rates dropped, remaining relatively low until the early 2000s. Then a transition took place starting in 2003, a dry and the warmest year in the series, when delivery rates are still relatively low, to relatively high values from 2005 onwards (only 2009 is markedly lower). A further increase occurs from 2011, the driest year in the series (see also Figure 6). This evolution suggests that climatologically exceptional years, i.e. dry and warm or wet and cold, can lead to an increase or decrease in sediment flux that persists over a longer-than-annual time-scale (Figure 12c). These changes can be associated with changes in geomorphic functioning of the catchment system, which may pertain sediment availability, system connectivity or transport capacity.

Figure 12d shows a similar plot of climate forcing on the measured annual water yield for the earlier defined periods. The correlation is less clear and less strong than for sediment supply (for the reference period $R^2 = 0.21$, $p < 0.02$). The periods here are much less distinct, emphasizing that it is probable that the more distinct periods in sediment delivery (Figure 12c) relate to differences in sediment access and connectivity. The periods in Figure 12d also show a progressive decrease in water yield with respect to the climate reference. If we take this one step further and take into account the evolution of transport capacity in the form of the SCR, the period since 2005 shows an even clearer increase in the effective sediment supply (Figure 12e). Interestingly, the differences between the reference period and the periods 1990-1994 and 1995-2004 are less distinct, suggesting a larger role for transport capacity here in the supply of sediment. The observations from Figure 12e however need to be taken with care as we determine bed load transport capacity just downstream of the intake and the local morphology is affected by purging as mentioned earlier. In general, the results illustrate the complexity and potentially large response of the proglacial margin in terms of sediment access and transfer. The direct response and sediment transfer here also support the observation of large transfer rates downstream of the intake.

5 Discussion

5.1 Morphological response to sediment supply and transfer

Widespread aggradation of up to 5 meters was found in the upstream braided reaches of the studied river since the introduction of flow abstraction and sediment purging in the early 1960s (Figure 7). An initial morphologic response was identified (in the period 1959-1965) although modest and short-lived, particularly compared to the aggradation that has occurred since the 1990s (Figure 8a). The following phase of morphologic evolution, between 1965 and the mid-1980s, is characterized by relatively low levels of net aggradation (Figure 8a). The river does however respond by channel narrowing, bar stabilization and vegetation encroachment (Figure 8b; 1977 orthoimage reach A in Supporting Information S1; see also Gurnell, 1983), which can be attributed to the reduced frequency of stream perturbing flows since the onset of flow abstraction. These changes appear to reflect the classic model of river response downstream of reservoir dams, where vegetation encroachment often occurs (Church, 1995; Petts & Gurnell 2005; Williams & Wolman 1984) even if in this case there was bed aggradation rather than degradation.

From the mid-1980s, and notably between 1988 and 1995, significant aggradation took place both through lateral channel expansion and an increase in bed level elevation (Figure 8). A similar transition in the pro-glacial channel upstream from the intake was noted by Warburton (1994). The aggradation was widespread, volumes comparable between the reaches studied, with only the upstream part of reach A receiving considerably larger amounts of sediment. The aggradation was accompanied by the steepening of reach-based bed gradients (Figure 8c) and to a lesser extent gradients in grain size (Figure 2). The greatest aggradation and coarsest sediment is found in the upstream part (or near upstream part in the case of reach A) of each reach. Here, sediment laden purges emerge from steeper and more confined reaches and are attenuated due to a decrease in channel gradient, an increase in flow width and are partially absorbed by the coarse and dry river bed (e.g. Buffington & Tonina 2009). This morphological signature may be typical for flow abstraction where sediment supply is maintained, most likely preventing the natural morphological evolution following from glacier recession and associated vegetation and ecological succession (Klaar et al., 2015). These results emphasize the observations of Wohl et al. (2015) and Gabbud & Lane (2016) that sediment regime needs to be factored into the design of river flows that might improve the ecological status of such streams.

The temporal changes in reach aggradation show little evidence for sequential morphologic response of the reaches (Figure 8a, 8b). A lag in sediment transfer and subsequent downstream propagation of a sediment wave (e.g. Nicholas et al., 1995) may be expected in this setting due to reduced transport conditions (Gabbud & Lane, 2016; Lane et al., 2014), but this is not apparent at the temporal resolution, between 4-6 years (with the exception of 1965-1977), of the topographic data. The dynamic river bed and relatively high transfer rates lead to rapid topographic change throughout the reaches in the 1980s (reach B) and more prominently in the early 1990s (reaches A, C and D). This change occurred in more or less direct response to increased sediment supply from higher up in the catchment relative to the (earlier) hydropower-reduced sediment transport capacity.

Despite there being a major reduction in sediment transport capacity due to flow abstraction (Figure 11b), the morphological evolution and downstream extent of aggradation indicate that sediment may still be transported through the river reaches (Figure 8a). Indeed, the evolution of the sediment supplied to the upstream reach A mirrors the sediment export from downstream reach D (Figure 9a), emphasizing that notwithstanding a substantial amount of sediment that was stored in the reaches since the onset of flow abstraction (Figure 7a), significant sediment transfer to downstream reaches is maintained. This is supported by similar trends in bed level aggradation and lateral expansion of the Borgne near Evolène and confidential gravel mining data from a site downstream. Particularly the finer fractions, if they are not abstracted with the water through the intake system, are expected to be transferred fairly efficiently downstream to the Rhône as flow increases (from tributaries with relatively low sediment loads) and the channel is generally constrained. This would suggest that the introduction of flow abstraction in the 1950s and 1960s (Park, 1980) may have had only a limited impact on decreasing suspended sediment loads in the same period (Loizeau & Dominik, 2000).

In general, our findings show that effects of flow abstraction schemes on downstream morphology and sediment transfer are distinctly different from those of classical reservoir dams. This difference can effectively be explained by the (designed) sediment storage capacity of these systems which leads to different timescales on which sediment flushing may take place: hourly to daily purging, in the case of sediment traps at flow intakes, or infrequent to no flushing at all, in the case of reservoir dams. This difference in sediment purging frequency together with the reduced flow, common to both flow intake and reservoir dam systems, then impacts on the natural channel dynamics and riparian ecology. In flow abstraction systems we typically find river bed aggradation with sediment throughput and ecological degeneration (Gabbud & Lane, 2016) as compared with downstream of reservoir dams where river bed degradation with sediment starvation and ecosystem stabilization has been observed (e.g. Petts & Gurnell 2005; Williams & Wolman 1984).

5.2 Climate forcing of sediment delivery

Climate has a strong impact on annual sediment delivery to the upper Borgne d'Arolla (Figure 12a-c). High summer temperatures allow for high rates of glacial melt, which simultaneously releases sediment and provides enhanced flow to transport that sediment (Lane et al., 2017). Preceding winter precipitation modulates this effect, where a thick snow cover may delay and shorten the period of summer ice melt. Despite significant flow abstraction, the system downstream of the intake is able to maintain significant sediment transfer (Figure 10b), which means that the climate signal is also propagated through the braided river reaches and potentially further through the basin. Indeed, the climate driven increase in glacial sediment export we found in the late 1980s to early 1990s corresponds with an increase in suspended sediment from the Upper Rhône basin as measured near the outlet into Lake Geneva (Costa et al., 2017).

Superimposed on annual variability, climatically exceptional years appear to have an indirect impact on a larger time-scale, of a few years to a decade, through forcing changes in upstream sediment dynamics (Figure 12c). The periodic changes shown in Figure 12c may relate to systematic changes in sediment availability and transfer within the proglacial margins of upstream glaciers, as they retreat rapidly. This is a process which initially releases sediment, in the early 1990s, and subsequently feedback processes may reduce that availability (Lane et al., 2017), although this reduction can at least in part be explained through reduced transport capacity (Figure 12e). From the mid-2000s there is a marked change in sediment supply, which can be related to supply from the HGdA and the retreating and thinning ice of the Bas Glacier. Initially, HGdA originating sediment that has previously accumulated under the Bas Glacier is released through improved connectivity following glacier recession, which may also explain a possible increase in fine sediment supply (Figure 9c). Later, sediment laden purges may more easily pass directly under the remaining ice. The latter coincides with the introduction of coordinated night-time purging of HGdA and LB intakes to enhance sediment output (Figure 4). Although these mechanisms and their contributions to sediment delivery can only be inferred here, the system evolution illustrates two important elements that may apply to Alpine systems in general. First, sediment connectivity in expanding pro-glacial areas is a key factor in the storage and export of sediment in these dynamic environments. Second, climate forcing and pro-glacial response may have a very large impact on sediment delivery, which in turn affects downstream sediment transfer and river bed morphology. Considering changes in local climate, sediment availability/release and connectivity (e.g. Lane et al., 2017), system evolution may vary strongly (both in time and between systems), making predictions with respect to the impacts of future climate change uncertain. On the long term however, climate warming and retreating glaciers will inevitably cause the decline of sediment yield from these catchments (e.g. Warburton, 1999).

5.3 Human forcing of system sensitivity

The introduction of flow abstraction has reduced discharge and bed load transport capacity in the upper Borgne d'Arolla by an estimated 95% (Figure 11a). Whilst transport capacity is reduced by 1-2 orders of magnitude, it is only reduced to close to the rates of sediment supply, with resulting SCR values that are not much larger than 1. This is not surprising as both the sediment supply and the residual sediment transport capacity are a function of the number of purges; flow (discharge and duration) are required to empty the sediment traps during purges. SCR values near 1 allow the sediment throughput through the system to be at least partly maintained. This is consistent with the rate and downstream gradient of river bed aggradation (Figure 8) and the significant sediment transfer that was maintained (Figure 10b).

The tendency for SCR values to be close to 1 due to flow abstraction means that the system has become highly sensitive to small changes in either sediment supply or sediment transport capacity. Due to this sensitivity, phases of external forcing, whether due to flow abstraction/regulation or climate change, can be distinguished in the morphological evolution of the Borgne. Initially, although little change occurred in the early stages following the onset of flow abstraction, the system dynamics and capacity to respond to external forcing did change. This only became apparent when a climate driven increase in sediment supply in the late 1980s and early 1990s led to an extensive aggradation (although there was still a large sediment transfer component). Similarly, since the early 2000s, there has been a general decrease in the capacity of the flow intake system to abstract high discharges (Figure 10a), leading to a sharp increase peak in flows associated with periods of (near) system surcharge (Figure 9c) since 2011. These are typically associated with high melt rates from glaciated basins during increasingly warm summers (Birsan et al., 2005) and high amounts of precipitation from convective storms (Giorgi et al., 2016). The resulting high flows from the LB catchment, in exceptional cases combined with flows from upstream catchments, are conveyed down the Borgne as longer duration, peak flow events. They are characterized by a high transport capacity and a relatively low sediment supply as compared to purges due to sediment trap flushing, where the use of water to purge the sediment traps is minimized for economic reasons. Further, the coordination of purges at the basin scale has led to routine night-time purges since 2008, where the LB intake is opened so as to allow purges from the upstream basins to pass through, resulting in elevated purges. Both of these changes are reflected in Figure 11a, where since 2003 there is a rising transport capacity, both in absolute and relative sense (with respect to the also increasing sediment supply), and an SCR that evolves towards 1 (Figure 11b). These high flow events can entrain sediment deposited downstream of the intake and potentially break armour layers, contributing to the substantial erosion of the upstream section of reach A (Figure 8a) and net export of sediment since 2010 (Figure 10b). In general, the system has become sensitive to high magnitude events, whether due to climate (e.g. high melt, convective storms), upstream events (e.g. glacial outburst floods) or human flow management (flow releases).

The key point here is that as flow abstraction has generally shifted the SCR towards one (Figure 11b), the system has become sensitive to relatively small changes in both climatically driven changes in sediment supply and how abstraction is managed, which can have major impacts on sediment transfer and river aggradation/degradation. This is exacerbated by legacy sediment (James, 2013), the accumulation of poorly sorted sediment downstream of the intakes, despite significant sediment throughput. The system sensitivity emphasizes the relevance of purge management, particularly the relative timing of purges from different intakes such that they coincide, optimizing sediment transfer and impacting morphological change. The capacity to which the hydropower system can be used to accommodate climate-driven upstream hydrological variability is however limited to the water intake and transfer capacity of the scheme, which effectively introduces a discharge threshold. The scheme was designed in a period of markedly cooler climate and lower water yield in the 1950s, which explains why it is now filled to capacity more frequently, leading to the need to reduce or stop water abstraction at the LB intake during peak flows. Thus, generalizing how flow abstraction in mountain environments impacts downstream sediment delivery and river morphodynamics needs to consider not only the direct impacts of abstraction and of climatic variability, but also how the water management system itself is coupled to that climatic variability.

6 Conclusions

In this study we used decadal scale river bed topographic change and hydropower impacted flow and sediment supply to analyze the evolution of river morphology and sediment transfer of an Alpine stream. The initial morphologic response to the onset of flow abstraction in 1963 was modest, generally associated with channel narrowing and vegetation encroachment. Major, widespread aggradation did not commence until the onset of glacier retreat in the late 1980s and the notably warm (and dry) period in the early 1990s. This aggradation coincided with a phase of increased sediment supply, although aggradation accounts for only circa 25% of supplied material and the remainder was transferred through the reaches downstream. Since the mid-2000s, a second phase of increased sediment supply was accompanied by an increased frequency of (near) system surcharge events due to insufficient intake system capacity, which led to the net export of sediment from the braided reaches. Based on the system evolution we can summarize the effects of flow abstraction and climate change on Alpine fluvial sediment transfer.

First, flow abstraction schemes for hydropower differ from classical reservoir dam schemes in that they ensure river sediment throughput through intermittent purges. Although flow abstraction may lead to a reduction in bed load transport capacity by 1-2 orders of magnitude, residual transport rates may still be sufficient to maintain significant sediment transfer. However, the sediment transfer rates and system morphological evolution then become much more sensitive both to internal river bed morphodynamics and external forcing mechanisms, whether natural or human induced. Because sediment transfer is largely maintained, the downstream morphological evolution of the stream is distinctly different from that downstream of reservoir dams. With low prevailing sediment supply, river bank stabilization and vegetation development encroachment occurs due to infrequent river perturbations and low flow competence. When this is met by a sufficiently high rate of sediment, aggradation will occur, leading to the removal or burial of vegetation. Maintained sediment supply and loss of transport capacity due to flow abstraction typically lead to a decreasing gradient in bed level rise and grain size.

Second, there is a climate forcing of river morphological response where rapid warming and associated glacial retreat lead to increased sediment availability and an adapting paraglacial landscape in which sediment may be stored and/or transferred. Climatic conditions directly impact annual sediment export not only through elevated summer temperatures, where ice melt leads to sediment release and enhanced transport conditions, but indirectly also through preceding winter snowfall, which may persist into the summer and buffer the effect of ice melt. Climate may also force changes in the pro-glacial margin, notably through sediment connectivity and access of sediment sources related to glacier retreat.

Third, human forcing and climate forcing may be strongly coupled, where the climate variability experienced by the river is conditioned by design and operation of the hydropower system. The capacity of flow releases from the intake to impact downstream sediment transfer is related to their nature, in this case individual sediment trap purges versus basin-wide coordinated purges and most notably (near) system surcharge events. The increasing occurrence of the latter is directly related to climate warming which leads to higher glacial melt rates while the capacity of the hydropower system, designed in a cooler period with lower water yield, is insufficient to accommodate these. This requires the prolonged opening of intakes (as compared to individual purges), allowing the climate driven peak flows to impact downstream sediment transfer and morphology. Thus besides the direct effect on upstream sediment delivery, climate change may have a profound impact on the operation of the hydropower system and hence also an indirect effect on downstream sediment dynamics. The individual effects of (human induced) climate forcing and direct human forcing through flow abstraction cannot be readily distinguished because the latter evolves continually in response to the former.

Alpine river basins are very sensitive to impacts of climate change. While their response in terms of sediment production and storage dynamics may be complex, we have shown that this may result in both rapid and strong increases in sediment delivery rates from pro-glacial margins. The sediment transport capacity and dynamics of subsequent mountain streams is such that, even when heavily impacted by flow regulation or even abstraction, they may transfer significant amounts of sediment down to main rivers. This implies that the potential impacts on infrastructure and ecology are not restricted to mountain headwaters but may affect the wider river basin and emphasizes the importance of sediment regime in river management.

Acknowledgements

This paper was written within the context of the SEDFATE project funded by the SNSF Sinergia grant CRSII2_147689, awarded to Fritz Schlunegger, Stéphanie Girardclos, Stuart Lane, Jean-Luc Loizeau and Peter Molnar. We thank SwissTopo for supplying scanned aerial photographs, Grande Dixence SA, Alpiq and Hydro Exploitation for providing discharge data, and Christoph Frei (MeteoSwiss) for providing spatially interpolated temperature and precipitation datasets. Additional support came from the students of the University of Lausanne, the Canton Valais, the Fondation Herbette and the Commune of Evolène. We would also like to thank the Associate Editor, David Morche and two anonymous reviewers for their detailed and constructive comments which have led to the improvement of this manuscript. Data concerning reach-based aggradation and annual sediment supply will be made available on http://ebibalpin.unil.ch/. For further information on the used data please contact Maarten Bakker (maarten.bakker@unil.ch) or Prof. Stuart Lane (stuart.lane@unil.ch).

References

Ashmore, P. & Church, M. (1998). Sediment transport and river morphology: a paradigm for study. *Water Resources Publications LLC, Highlands Ranch, Colorado*, 115-148.

Badoux, A., Andres, N. & Turowski, J. (2014). Damage costs due to bedload transport processes in Switzerland. *Natural Hazards and Earth System Science, 14*(2), 279-294. doi: 10.5194/nhess-14-279-2014

Bakker, M. & Lane, S. N. (2017). Archival photogrammetric analysis of river–floodplain systems using Structure from Motion (SfM) methods. *Earth Surface Processes and Landforms, 42*(8), 1274-1286. doi:10.1002/esp.4085

Ballantyne, C. K. (2002). A general model of paraglacial landscape response. *The Holocene, 12*(3), 371-376. doi:10.1191/0959683602hl553fa

Beniston, M., Rebetez, M., Giorgi, F. & Marinucci, M. R. (1994). An analysis of regional climate change in Switzerland. *Theoretical and Applied Climatology, 49*(3), 135-159. doi:10.1007/bf00865530

Bezinge, A., Clark, M., Gurnell, A. & Warburton, J. (1989). The management of sediment transported by glacial melt -water streams and its significance for the estimation of sediment yield. *Annals of Glaciology, 13*, 1-5. doi:10.1017/S0260305500007527

Birsan, M.-V., Molnar, P., Burlando, P. & Pfaundler, M. (2005). Streamflow trends in Switzerland. *Journal of Hydrology, 314*(1–4), 312-329. doi:10.1016/j.jhydrol.2005.06.008

Brasington, J., Langham, J. & Rumsby, B. (2003). Methodological sensitivity of morphometric estimates of coarse fluvial sediment transport. *Geomorphology, 53*(3–4), 299-316. doi:10.1016/S0169-555X(02)00320-3

Buffington, J. M. & Tonina, D. (2009). Hyporheic Exchange in Mountain Rivers II: Effects of Channel Morphology on Mechanics, Scales, and Rates of Exchange. *Geography Compass, 3*(3), 1038-1062. doi:10.1111/j.1749-8198.2009.00225.x

Carbonneau, P. E., Lane, S. N. & Bergeron, N. E. (2004). Catchment-scale mapping of surface grain size in gravel bed rivers using airborne digital imagery. *Water Resources Research, 40*(7). doi: 10.1029/2003WR002759

Ceppi, P., Scherrer, S. C., Fischer, A. M. & Appenzeller, C. (2012). Revisiting Swiss temperature trends 1959–2008. *International Journal of Climatology, 32*(2), 203-213. doi:10.1002/joc.2260

Church, M. (1995). Geomorphic response to river flow regulation: case studies and time-scales. *Regulated Rivers-Research and Management, 11*(1), 3-22. doi: 10.1002/rrr.3450110103

Church, M. (2006). Bed material transport and the morphology of alluvial river channels. *Annu. Rev. Earth Planet. Sci., 34*, 325-354. doi: 10.1146/annurev.earth.33.092203.122721

Church, M. & Ryder, J. M. (1972). Paraglacial sedimentation: a consideration of fluvial processes conditioned by glaciation. *Geological Society of America Bulletin, 83*(10), 3059-3072. doi: 10.1130/0016-7606(1972)83[3059:PSACOF]2.0.CO;2

Cossart, E. & Fort, M. (2008). Sediment release and storage in early deglaciated areas: Towards an application of the exhaustion model from the case of Massif des Écrins (French Alps) since the Little Ice Age. *Norsk Geografisk Tidsskrift - Norwegian Journal of Geography, 62*(2), 115-131. doi:10.1080/00291950802095145

Costa, A., Molnar, P., Stutenbecker, L., Bakker, M., Silva, T. A., Schlunegger, F., . . . Girardclos, S. (2017). Temperature signal in suspended sediment export from an Alpine catchment. *Hydrol. Earth Syst. Sci. Discuss., 2017*, 1-30. doi:10.5194/hess-2017-2

Curry, A. M., Cleasby, V. & Zukowskyj, P. (2006). Paraglacial response of steep, sediment-mantled slopes to post-'Little Ice Age' glacier recession in the central Swiss Alps. *Journal of Quaternary Science, 21*(3), 211-225. doi:10.1002/jqs.954

Fergus, T. (1997). Geomorphological response of a river regulated for hydropower: River Fortun, Norway. *Regulated Rivers: Research & Management, 13*(5), 449-461. doi:10.1002/(SICI)1099-1646(199709/10)13:5<449::AID-RRR468>3.0.CO;2-#

Ferguson, R. (2007). Flow resistance equations for gravel- and boulder-bed streams. *Water Resources Research, 43*(5), W05427. doi:10.1029/2006wr005422

Fischer, L., Huggel, C., Kääb, A. & Haeberli, W. (2013). Slope failures and erosion rates on a glacierized high-mountain face under climatic changes. *Earth Surface Processes and Landforms, 38*(8), 836-846. doi:10.1002/esp.3355

Frei, C. (2014). Interpolation of temperature in a mountainous region using nonlinear profiles and non-Euclidean distances. *International Journal of Climatology, 34*(5), 1585-1605. doi:10.1002/joc.3786

Gabbud, C. & Lane, S. N. (2016). Ecosystem impacts of Alpine water intakes for hydropower: the challenge of sediment management. *Wiley Interdisciplinary Reviews: Water, 3*(1), 41-61. doi:10.1002/wat2.1124

Geilhausen, M., Morche, D., Otto, J.-C. & Schrott, L. (2013). Sediment discharge from the proglacial zone of a retreating Alpine glacier. *Zeitschrift für Geomorphologie, Supplementary Issues, 57*(2), 29-53. doi: 10.1127/0372-8854/2012/S-00122

Giorgi, F., Hurrell, J. W., Marinucci, M. R. & Beniston, M. (1997). Elevation Dependency of the Surface Climate Change Signal: A Model Study. *Journal of Climate, 10*(2), 288-296. doi:10.1175/1520-0442(1997)010<0288:EDOTSC>2.0.CO;2

Giorgi, F., Torma, C., Coppola, E., Ban, N., Schar, C. & Somot, S. (2016). Enhanced summer convective rainfall at Alpine high elevations in response to climate warming. *Nature Geosci, advance online publication*. doi:10.1038/ngeo2761

Glaciological Reports (1881-2017). "The Swiss Glaciers", Yearbooks of the Cryospheric Commission of the Swiss Academy of Sciences (SCNAT). http://www.glamos.ch.

Gobiet, A., Kotlarski, S., Beniston, M., Heinrich, G., Rajczak, J. & Stoffel, M. (2014). 21st century climate change in the European Alps—A review. *Science of The Total Environment, 493*, 1138-1151. doi: 10.1016/j.scitotenv.2013.07.050

Gruber, S. & Haeberli, W. (2007). Permafrost in steep bedrock slopes and its temperature-related destabilization following climate change. *Journal of Geophysical Research: Earth Surface, 112*(F2). doi:10.1029/2006JF000547

Gurnell, A. (1983). Downstream channel adjustments in response to water abstraction for hydro-electric power generation from alpine glacial melt-water streams. *The Geographical Journal, 149*(3), 342-354. doi:10.2307/634009

Gurnell, A., Warburton, J. & Clark, M. 1988. A comparison of the sediment transport and yield characteristics of two adjacent glacier basins, Val d' Herens, Switzerland. In Sediment Budgets (Proceedings Porto Alegre Symposium December 1988) IAHS Publication 174, 431-441.

Haeberli, W. & Beniston, M. (1998). Climate change and its impacts on glaciers and permafrost in the Alps. *Ambio*, 258-265.

Haeberli, W., Hoelzle, M., Paul, F. & Zemp, M. (2007). Integrated monitoring of mountain glaciers as key indicators of global climate change: the European Alps. *Annals of Glaciology, 46*(1), 150-160. doi:10.3189/172756407782871512

Harbor, J. & Warburton, J. (1993). Relative Rates of Glacial and Nonglacial Erosion in Alpine Environments. *Arctic and Alpine Research, 25*(1), 1-7. doi:10.2307/1551473

Heckmann, T., McColl, S. & Morche, D. (2016). Retreating ice: research in pro-glacial areas matters. *Earth Surface Processes and Landforms, 41*(2), 271-276. doi:10.1002/esp.3858

Hilker, N., Badoux, A. & Hegg, C. (2009). The Swiss flood and landslide damage database 1972–2007. *Nat. Hazards Earth Syst. Sci, 9*(3), 913-925. doi:nhess-9-913-2009_lq

Hinderer, M., Kastowski, M., Kamelger, A., Bartolini, C. & Schlunegger, F. (2013). River loads and modern denudation of the Alps — A review. *Earth-Science Reviews, 118*(0), 11-44. doi:10.1016/j.earscirev.2013.01.001

Holm, K., Bovis, M. & Jakob, M. (2004). The landslide response of alpine basins to post-Little Ice Age glacial thinning and retreat in southwestern British Columbia. *Geomorphology, 57*(3–4), 201-216. doi:10.1016/S0169-555X(03)00103-X

Hunziker, R. P. & Jäggi, M. N. R. (2002). Grain Sorting Processes. *Journal of Hydraulic Engineering 128*(12), 1060-1068. doi:10.1061/(ASCE)0733-9429(2002)128:12(1060)

James, L. A. (2013). Legacy sediment: Definitions and processes of episodically produced anthropogenic sediment. *Anthropocene, 2*, 16-26. doi:10.1016/j.ancene.2013.04.001

Klaar, M. J., Kidd, C., Malone, E., Bartlett, R., Pinay, G., Chapin, F. S. & Milner, A. (2015). Vegetation succession in deglaciated landscapes: implications for sediment and landscape stability. *Earth Surface Processes and Landforms, 40*(8), 1088-1100. doi:10.1002/esp.3691

Lane, S. N., Bakker, M., Balin, D., Lovis, B. & Regamey, B. (2014). Climate and human forcing of Alpine river flow. In A. J. Schleiss, G. de Cesare, M. J. Franca & M. Pfister (Eds.), *River Flow 2014*, 7-15.

Lane, S. N., Bakker, M., Gabbud, C., Micheletti, N. & Saugy, J.-N. (2017). Sediment export, transient landscape response and catchment-scale connectivity following rapid climate warming and Alpine glacier recession. *Geomorphology, 277*, 210-227. doi:10.1016/j.geomorph.2016.02.015

Lane, S. N., Reid, S. C., Westaway, R. M. & Hicks, D. M. (2004). Remotely Sensed Topographic Data for River Channel Research: The Identification, Explanation and Management of Error. In R. E. J. Kelly, N. A. Drake & S. L. Barr (Eds.), *Spatial modelling of the terrestrial environment,* John Wiley & Sons, Ltd, 113-136.

Lane, S. N., Richards, K. S., & Chandler, J. H. (1994). Developments in monitoring and modelling small-scale river bed topography. Earth Surface Processes and Landforms, 19(4), 349-368. doi:10.1002/esp.3290190406

Lane, S. N., Tayefi, V., Reid, S. C., Yu, D. & Hardy, R. J. (2007). Interactions between sediment delivery, channel change, climate change and flood risk in a temperate upland environment. *Earth Surface Processes and Landforms, 32*(3), 429-446. doi:10.1002/esp.1404

Lane, S. N., Westaway, R. M. & Murray Hicks, D. (2003). Estimation of erosion and deposition volumes in a large, gravel-bed, braided river using synoptic remote sensing. *Earth Surface Processes and Landforms, 28*(3), 249-271. doi:10.1002/esp.483

Lindsay, J. B., & Ashmore, P. E. (2002). The effects of survey frequency on estimates of scour and fill in a braided river model. Earth Surface Processes and Landforms, 27(1), 27-43. doi:10.1002/esp.282

Loizeau, J.-L. & Dominik, J. (2000). Evolution of the Upper Rhone River discharge and suspended sediment load during the last 80 years and some implications for Lake Geneva. *Aquatic Sciences, 62*(1), 54-67. doi:10.1007/s000270050075

Margot, A., Schädler, B., Sigg, R. & Weingartner, R. (1992). Influence on rivers by water power stations (> 300 kW) and the lake control. *Hydrological Atlas of Switzerland. Plate, 5*.

MeteoSwiss (2016a). Daily Mean, Minimum and Maximum Temperature: TabsD, TminD, TmaxD. http://www.meteoswiss.admin.ch/content/dam/meteoswiss/de/service-und-publikationen/produkt/raeumliche-daten-temperatur/doc/ProdDoc_TabsD.pdf

MeteoSwiss (2016b). Daily Precipitation (final analysis): RhiresD. http://www.meteoswiss.admin.ch/content/dam/meteoswiss/de/service-und-publikationen/produkt/raeumliche-daten-niederschlag/doc/ProdDoc_RhiresD.pdf

Micheletti, N., Lambiel, C. & Lane, S. N. (2015). Investigating decadal-scale geomorphic dynamics in an alpine mountain setting. *Journal of Geophysical Research: Earth Surface, 120*(10), 2155-2175. doi:10.1002/2015JF003656

Micheletti, N. & Lane, S. N. (2016). Water yield and sediment export in small, partially glaciated Alpine watersheds in a warming climate. *Water Resources Research, 52*(6), 4924-4943. doi:10.1002/2016WR018774

Nicholas, A., Ashworth, P., Kirkby, M., Macklin, M. & Murray, T. (1995). Sediment slugs: large-scale fluctuations in fluvial sediment transport rates and storage volumes. *Progress in physical geography, 19*(4), 500-519.

Nitsche, M., Rickenmann, D., Turowski, J. M., Badoux, A. & Kirchner, J. W. (2011). Evaluation of bedload transport predictions using flow resistance equations to account for macro-roughness in steep mountain streams. *Water Resources Research, 47*(8), W08513. doi:10.1029/2011WR010645

Norton, K. P., Abbühl, L. M. & Schlunegger, F. (2010). Glacial conditioning as an erosional driving force in the Central Alps. *Geology, 38*(7), 655-658. doi:10.1130/G31102.1

Park, C. (1980). The Grande Dixence hydro-electric scheme, Switzerland. *Geography*, 317-320.

Paul, F., Kääb, A., Maisch, M., Kellenberger, T. & Haeberli, W. (2004). Rapid disintegration of Alpine glaciers observed with satellite data. *Geophysical Research Letters, 31*(21). doi:10.1029/2004GL020816

Petts, G. E. & Bickerton, M. A. (1994). Influence of water abstraction on the macroinvertebrate community gradient within a glacial stream system: La Borgne d'Arolla, Valais, Switzerland. *Freshwater Biology, 32*(2), 375-386. doi:10.1111/j.1365-2427.1994.tb01133.x

Petts, G. E. & Gurnell, A. M. (2005). Dams and geomorphology: research progress and future directions. *Geomorphology, 71*(1), 27-47. doi: 10.1016/j.geomorph.2004.02.015

Raymond Pralong, M., Turowski, J. M., Rickenmann, D. & Zappa, M. (2015). Climate change impacts on bedload transport in alpine drainage basins with hydropower exploitation. *Earth Surface Processes and Landforms, 40*(12), 1587-1599. doi:10.1002/esp.3737

Rey, Y. & Dayer, G. (1990). Crues de l'été 1987 dans les bassins versants glaciaires des Alpes Pennines. *Revue de géographie alpine, 78*(1), 115-124.

Rickenmann, D. (1991). Hyperconcentrated flow and sediment transport at steep slopes. *Journal of Hydraulic Engineering, 117*(11), 1419-1439. doi: 10.1061/(ASCE)0733-9429(1991)117:11(1419)

Schar, C., Vidale, P. L., Luthi, D., Frei, C., Haberli, C., Liniger, M. A. & Appenzeller, C. (2004). The role of increasing temperature variability in European summer heatwaves. *Nature, 427*(6972), 332-336. doi:10.1038/nature02300

Small, R. J. (1973). Braiding terraces in the Val d'Herens, Switzerland. *Geography*, 129-135.

Stoffel, M. & Huggel, C. (2012). Effects of climate change on mass movements in mountain environments. *Progress in physical geography, 36*(3), 421-439. doi: 10.1177/0309133312441010

SwissTopo (1946). Aerial images swisstopo oblique (swisstopo): Picture number: 19461071550811, https//:map.geo.admin.ch

Tanchev, L. (2014). *Dams and appurtenant hydraulic structures*: CRC Press.

Turowski, J. M. & Rickenmann, D. (2009). Tools and cover effects in bedload transport observations in the Pitzbach, Austria. *Earth Surface Processes and Landforms, 34*(1), 26-37. doi:10.1002/esp.1686

Warburton, J. (1990). An alpine proglacial fluvial sediment budget. Geografiska Annaler. Series A. Physical Geography, 261-272. doi: 10.2307/521154

Warburton, J. (1992). Observations of bed load transport and channel bed changes in a proglacial mountain stream. Arctic and & Alpine Research, 24(3), 195-203. doi:10.2307/1551657

Warburton, J. (1994). Channel change in relation to meltwater flooding, Bas Glacier d'Arolla, Switzerland. *Geomorphology*, 11(2), 141-149. doi:https://doi.org/10.1016/0169-555X(94)90078-7

Warburton, J. (1999). Environmental change and sediment yield from glacierised basins: the role of fluvial processes and sediment storage (Chapter 19). In Brown, A.G. and Quine, T.A. (Eds.) *Fluvial Processes and Environmental Change*, Wiley, Chichester, 363-384.

Warburton, J. & Fenn, C. (1994). Unusual flood events from an Alpine glacier: observations and deductions on generating mechanism. *Journal of Glaciology, 40*(134), 176-186. doi: 10.1017/S0022143000003956

Wheaton, J. M., Brasington, J., Darby, S. E., Kasprak, A., Sear, D. & Vericat, D. (2013). Morphodynamic signatures of braiding mechanisms as expressed through change in sediment storage in a gravel-bed river. *Journal of Geophysical Research: Earth Surface, 118*(2), 759-779. doi:10.1002/jgrf.20060

Wheaton, J. M., Brasington, J., Darby, S. E. & Sear, D. A. (2010). Accounting for uncertainty in DEMs from repeat topographic surveys: improved sediment budgets. *Earth Surface Processes and Landforms, 35*(2), 136-156. doi:10.1002/esp.1886

Williams, G. P. & Wolman, M. G. (1984). *Downstream effects of dams on alluvial rivers*: US Government Printing Office Washington, DC.

Wohl, E., Bledsoe, B. P., Jacobson, R. B., Poff, N. L., Rathburn, S. L., Walters, D. M. & Wilcox, A. C. (2015). The Natural Sediment Regime in Rivers: Broadening the Foundation for Ecosystem Management. *BioScience, 65*(4), 358-371. doi:10.1093/biosci/biv002

Wold, B. & Østrem, G. (1979). Morphological activity of a diverted glacier stream in Western Norway. *GeoJournal, 3*(4), 345-349.

Wolman, M. G. (1954). A method of sampling coarse river-bed material. *Eos, Transactions American Geophysical Union, 35*(6), 951-956.

Tables

Year	Scale [1 :x]	Ground resolution [m]	RMSE bundle adjustment [m]
1959	23200	0.49	±0.34
1965	21200	0.45	±0.45
1977	19600	0.27	±0.20
1983	19600	0.27	±0.23
1988	20900	0.29	±0.21
1995	26800	0.38	±0.32
1999	27000	0.38	±0.44
2005	24700	0.35	±0.38
2010*	-	0.50	-
2014	13900	0.09	±0.12

Table 1 Summary of historical aerial photographs, processed using SfM photogrammetric methods, and derived bundle adjustment quality (from Bakker & Lane, 2017). *ALTI3D laser scan data SwissTopo.

Figure captions

Figure 1 a) Overview of Val d'Hérens showing the Borgne River and the downstream part of the Grande Dixence hydropower network; b) The pro-glacial river reach of the Borgne d'Arolla is fed by the Bas Glacier d'Arolla (1987 maximum extent indicated) and purges from the Haut Glacier d'Arolla (HGdA), Upper Bertol (UB) and Vuibé (VU) intakes. The Lower Bertol (LB) intake lies just upstream of reach A. The cross section (CS) is used for bed load transport capacity calculations; c) Reach B receives flow from reach A that has passed through a narrow, incised reach and from the Tsijiore Nouve (TN) tributary. Reaches C and D receive flow from reach B that has passed through another narrow, incised reach. Images are from 2009 (Google Earth); a scale indication is included in a) but decreases in downstream direction due to oblique imagery.

Figure 2 Long profile downstream from the Lower Bertol (LB) intake with average gradient and grain size D_{50} and D_{84} based on the 2014 DEM and orthoimage (a 200m averaging window was applied to emphasize reach-scale trends). The cross section where bed load transport capacity calculations were performed is indicated.

Figure 3 a) Intake discharge and estimated total discharge for two purges; b) Break in slope in the frequency distribution of discharge drawdowns; year 2006.

Figure 4 Discharge relation between Haut Glacier d'Arolla (HGdA) and Lower Bertol (LB) intakes during coincident purges (purges HGdA) and non-coincident purges (purges LB); period 2008-2013.

Figure 5 Cumulative distribution of the water volume releases as identified from 15-minute data in 2014 (197 purges in total) and minute data in 2015 (May-November 2015, 313 purges in total), which forms the basis to distinguish between sand trap purges, gravel trap purges and (near) system surcharge events.

Figure 6 a) Annual and summer (July – September) temperature; b) annual and winter (January – May) precipitation. Values are spatially interpolated for the Bas Glacier based on Frei (2014) and given as deviation from the mean of the whole period.

Figure 7 DEM of difference and river bed extent for the period 1959-2014 (background is a hillshade of the 2014 DEM). *The theoretical limit of detection is given but the actual values vary based on the constituent orthoimage entropies. Arrows indicate flow direction.

Figure 8 Long profiles showing channel change with respect to 1959 in: a) volume; b) sedimentation width; c) elevation. A 200 m averaging window was applied to emphasize reach-scale trends. Note that for a) and c) only values that exceed the detection limit are shown.

Figure 9 a) Annual water yield at the LB intake and the residual water yield (mainly purges) from the upstream HGdA intake - note that the latter is a factor 10 smaller; b) calculated (range in) sediment supply at the LB intake and HGdA intake and; (c) identified purges per type at the LB intake: sand trap, gravel trap, night-time purge (gravel trap), and (near) system surcharge events. The uncertainty range in LB water yield due to system surcharge is too small to be visible in a). The uncertainties in purge identification and sediment volume are reflected in the range in supply values in b). Data from HGdA is based on Lane et al. (2017).

Figure 10 a) Sediment transfer rate as absolute value and; b) sediment transfer as percentage: sediment exported from the reach divided by sediment supply to the reach. The annual values are averaged for periods between the available aerial photographs. The given ranges reflect uncertainties in sediment supply and, in the case of reaches B, C, D, uncertainties regarding the possible sediment transfer from the TN intake; uncertainties in reach storage are negligible.

Figure 11 a) Discharge reduction due to flow intake for total discharge and discharges exceeded for durations ranging from 2 days to 1 hour per year; b) Supply-Capacity Ratio (SCR) for residual flow and total flow: The ‘morphology range’ reflects the calculated range in transport capacity related to (temporal) changes in cross section with a constant (maximum) sediment supply (see Supporting Information S6); where the year and applied cross section correspond, the SCR values are plotted as a point (temporal changes in grain size are not accounted for). The ‘supply range’ reflects the uncertainty in sediment supply with the transport capacity based on the 2014 cross section. ‘Flow management’ reflects the effect of coinciding purges from HGdA and LB intakes on transport capacity based on the 2014 cross section. The SCR for total flow includes the uncertainty in sediment supply and the transport capacity based on the 2014 cross section.

Figure 12 Climate forcing of sediment supply and discharge; a) correlation summer temperature and sediment supply; b) correlation winter precipitation and sediment supply. Correlation ‘climate’ principal component with: c) sediment supply; d) water yield (2015 is not included due to the incomplete discharge series) and; e) Supply-Capacity Ratio (SCR), where the bed load transport capacity of the total discharge downstream of the intake is used. Exceptional years are marked (e.g. 11 is 2011) and the regression line, R^2, p value and 80 percentiles are based on the reference period 1977-1990.

Figure 1.

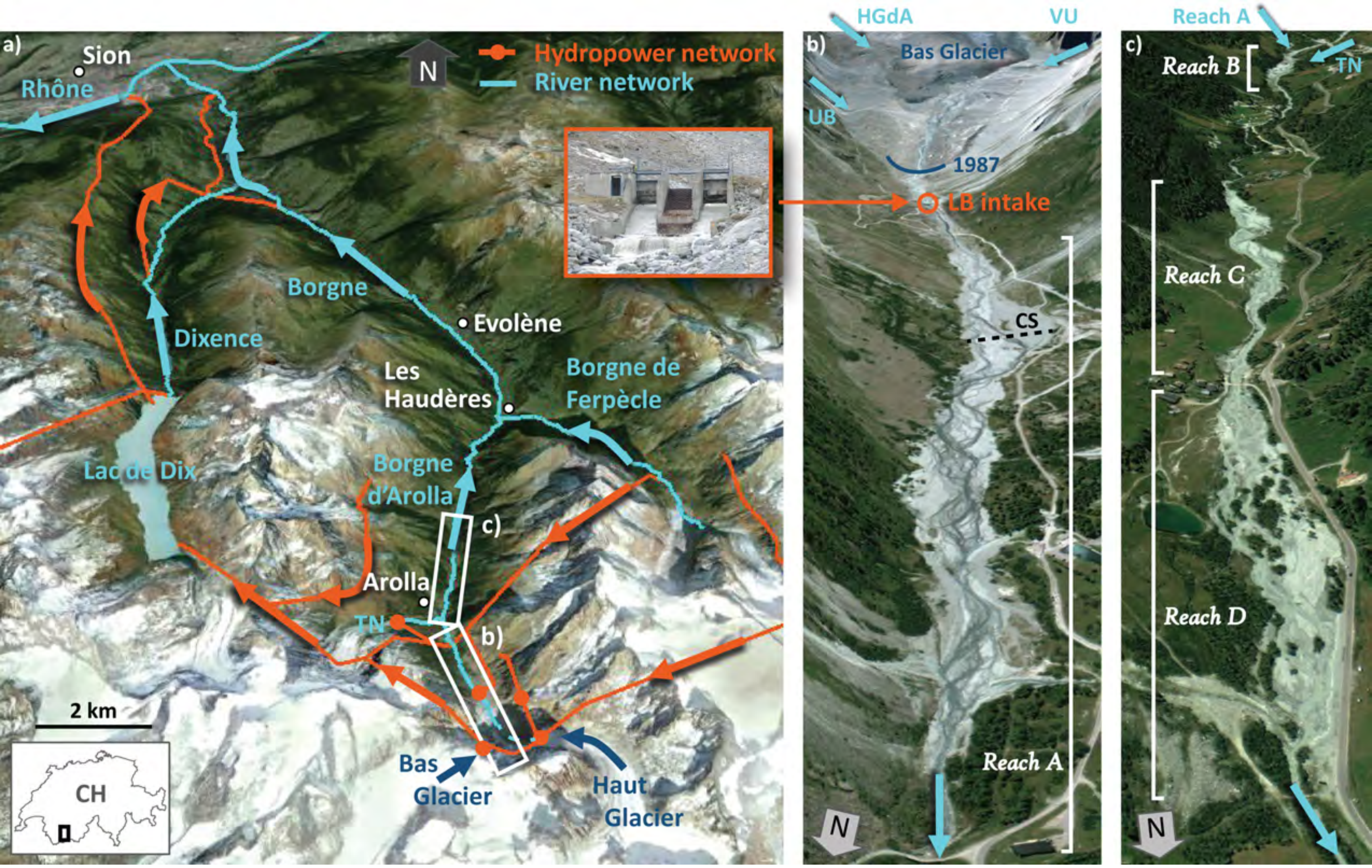

a)
Sion
Rhône
N
Hydropower network
River network
Borgne
Evolène
Dixence
Les Haudères
Borgne de Ferpècle
Lac de Dix
Borgne d'Arolla
c)
Arolla
TN
b)
2 km
CH
Bas Glacier
Haut Glacier
b)
HGdA
VU
Bas Glacier
UB
1987
LB intake
CS
Reach A
N
c)
Reach A
Reach B
TN
Reach C
Reach D
N

Figure 2.

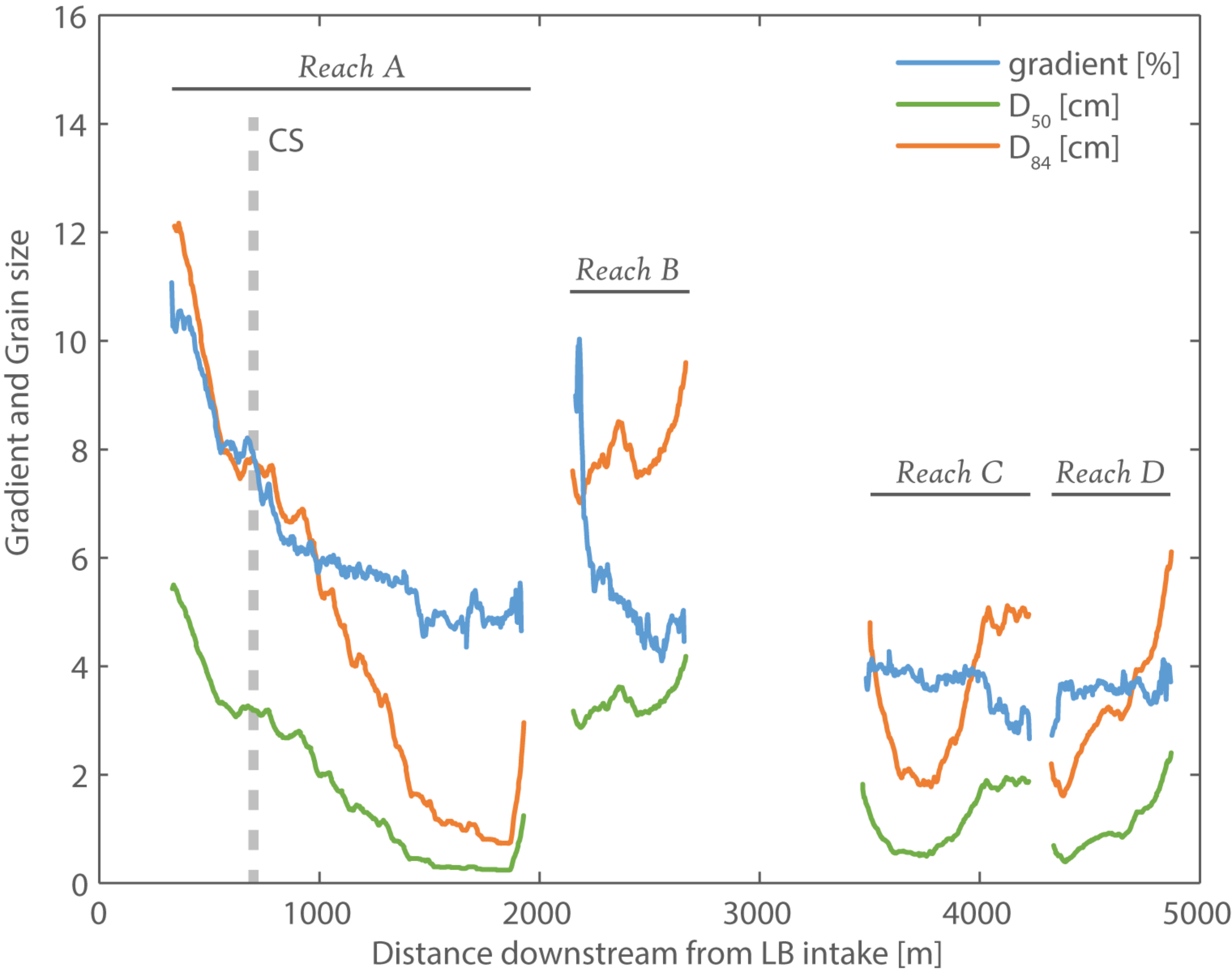

Reach A
Reach B
Reach C
Reach D
CS
gradient [%]
D50 [cm]
D84 [cm]
Gradient and Grain size
Distance downstream from LB intake [m]
0
2
4
6
8
10
12
14
16
0
1000
2000
3000
4000
5000

Figure 3.

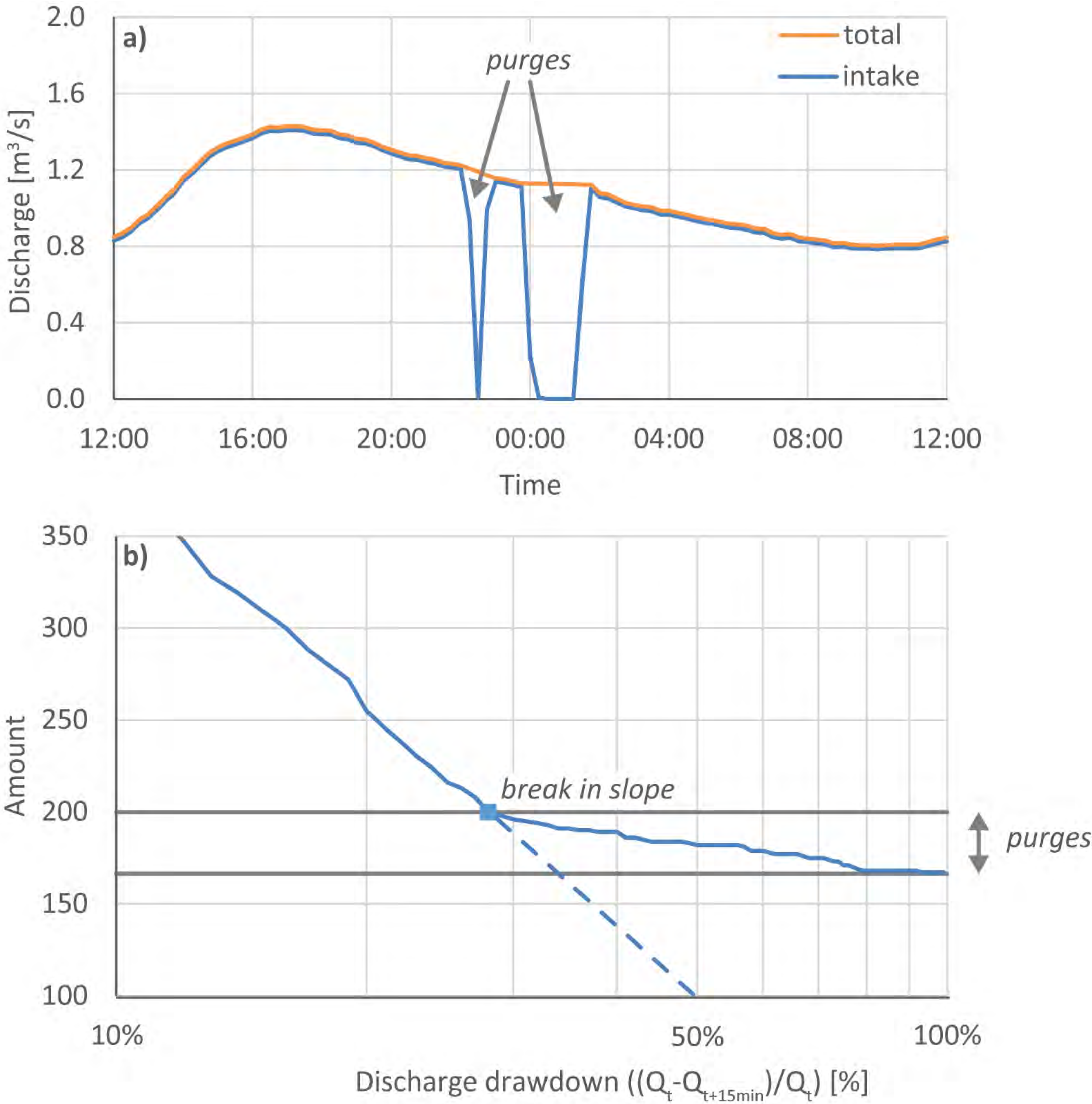

a)
total
intake
purges
Discharge [m³/s]
2.0
1.6
1.2
0.8
0.4
0.0
12:00
16:00
20:00
00:00
04:00
08:00
12:00
Time
b)
break in slope
purges
Amount
350
300
250
200
150
100
10%
50%
100%
Discharge drawdown ((Qt-Qt+15min)/Qt) [%]

Figure 4.

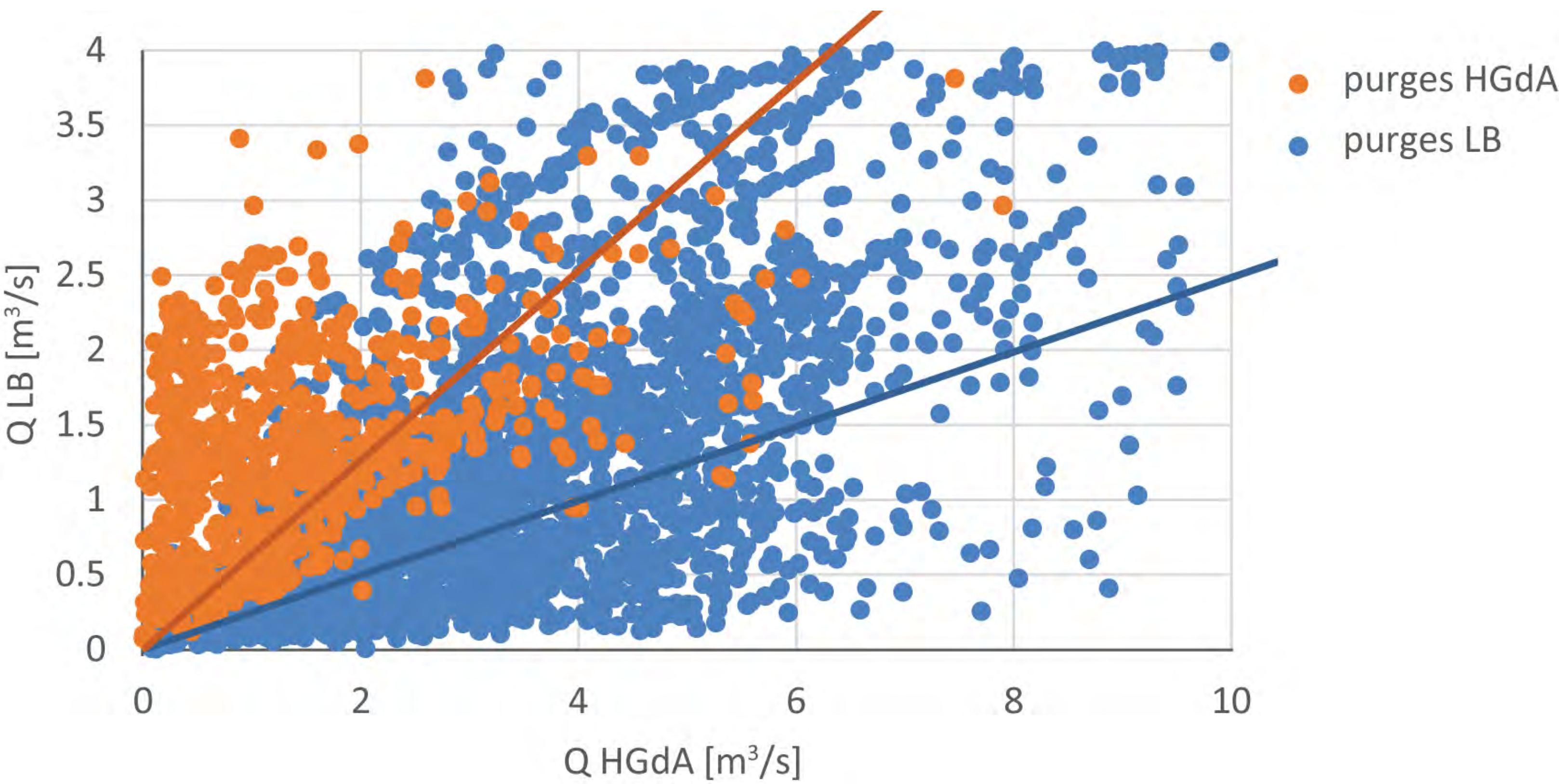

purges HGdA
purges LB
Q LB [m³/s]
Q HGdA [m³/s]
0
0.5
1
1.5
2
2.5
3
3.5
4
0
2
4
6
8
10

Figure 5.

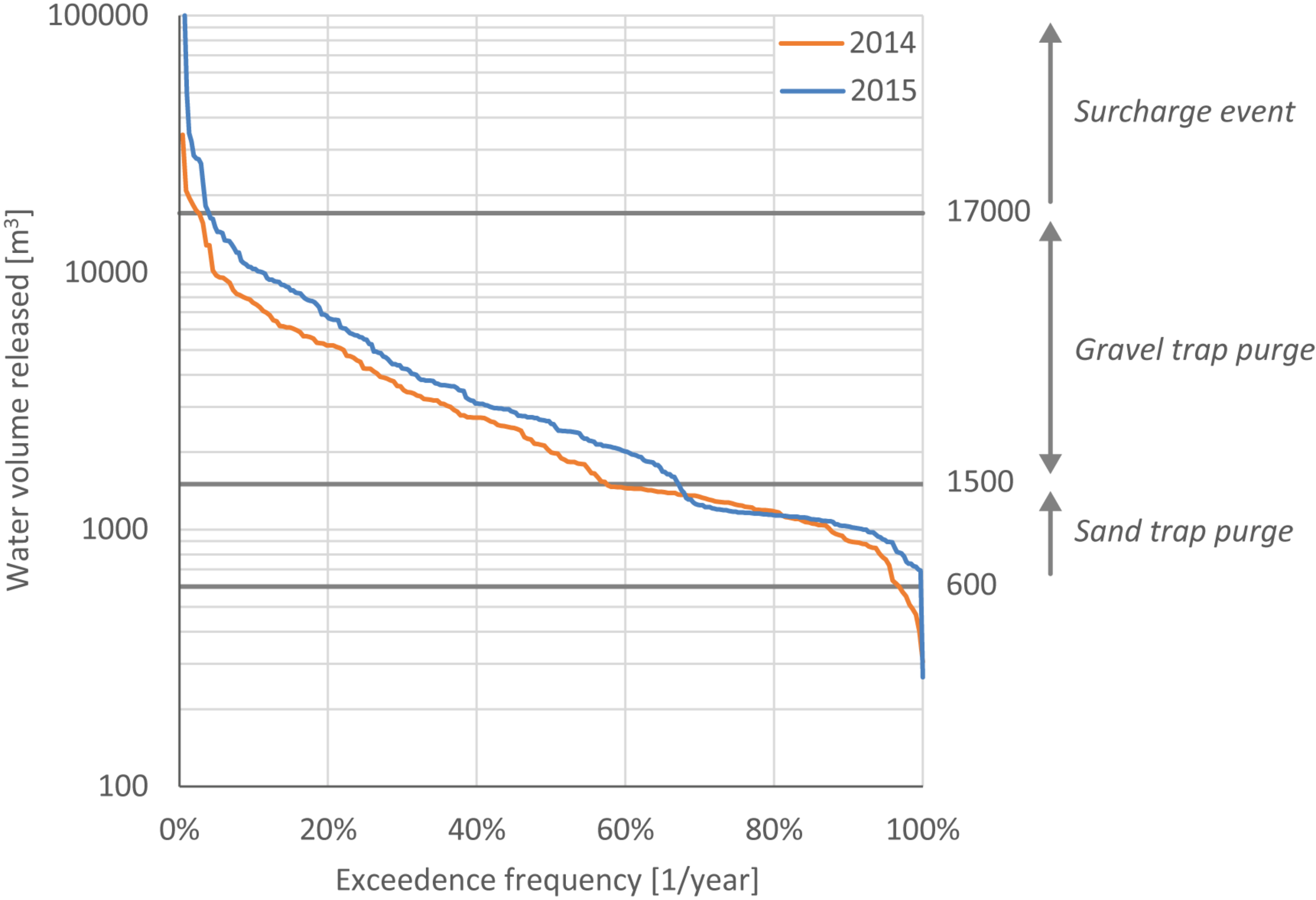
100000
10000
1000
100
Water volume released [m3]
0%
20%
40%
60%
80%
100%
Exceedence frequency [1/year]
2014
2015
17000
1500
600
Surcharge event
Gravel trap purge
Sand trap purge

Figure 6.

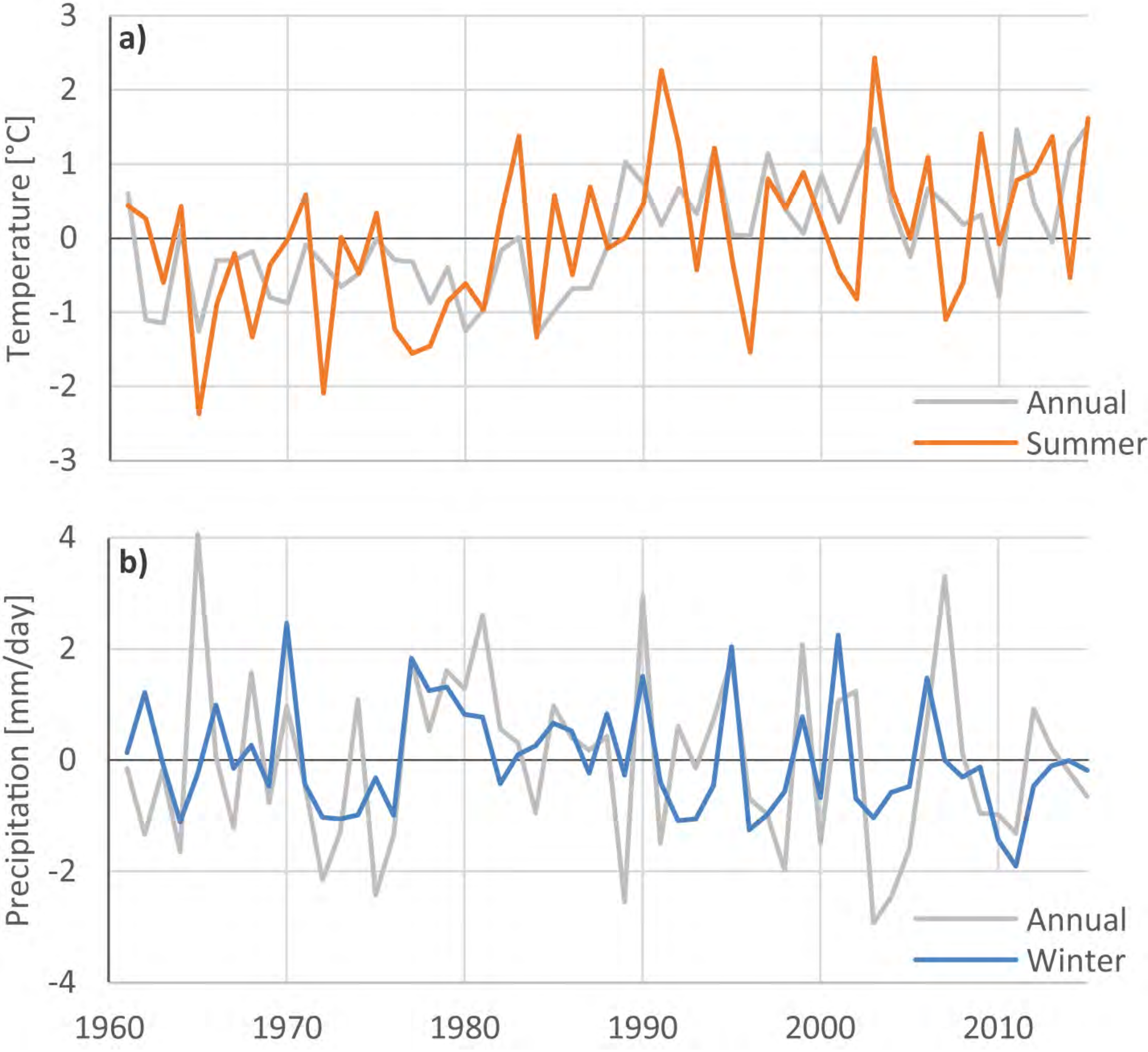
a)
b)
Temperature [°C]
Precipitation [mm/day]
Annual
Summer
Annual
Winter
3
2
1
0
-1
-2
-3
4
2
0
-2
-4
1960
1970
1980
1990
2000
2010

Figure 7.

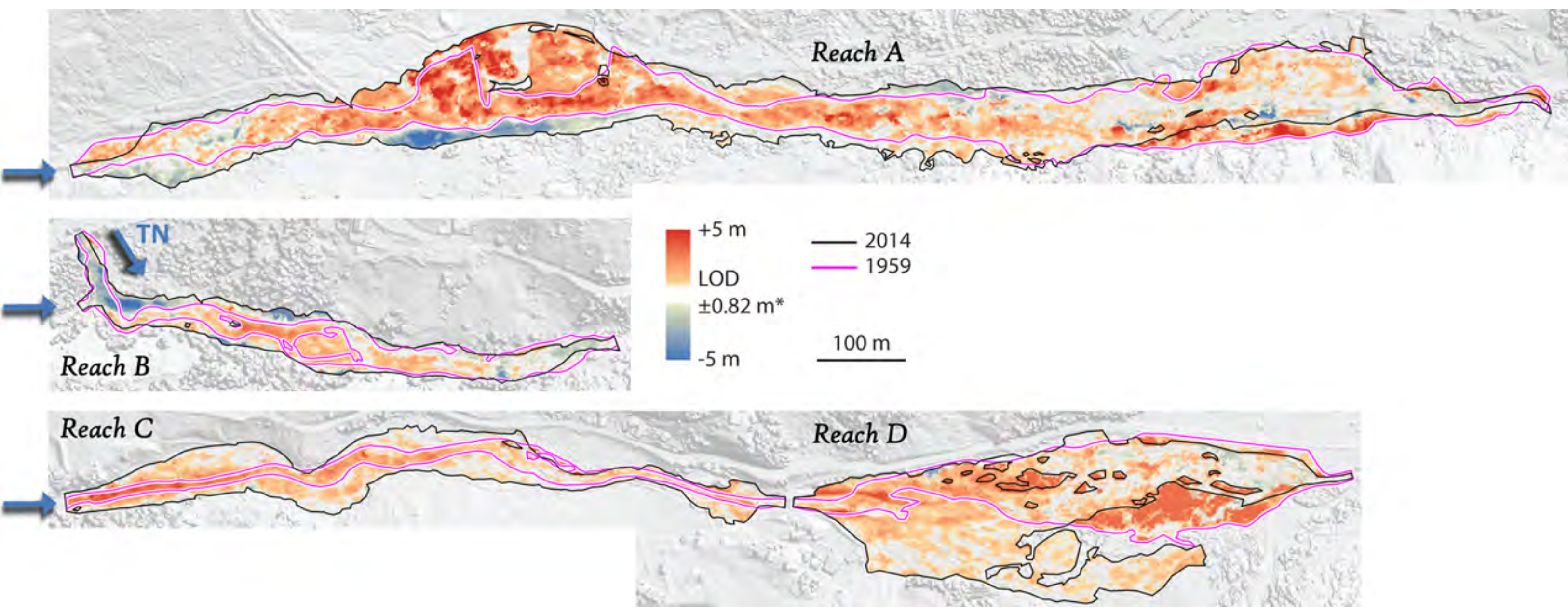
Reach A
TN
Reach B
+5 m
LOD
±0.82 m*
-5 m
2014
1959
100 m
Reach C
Reach D

Figure 8.

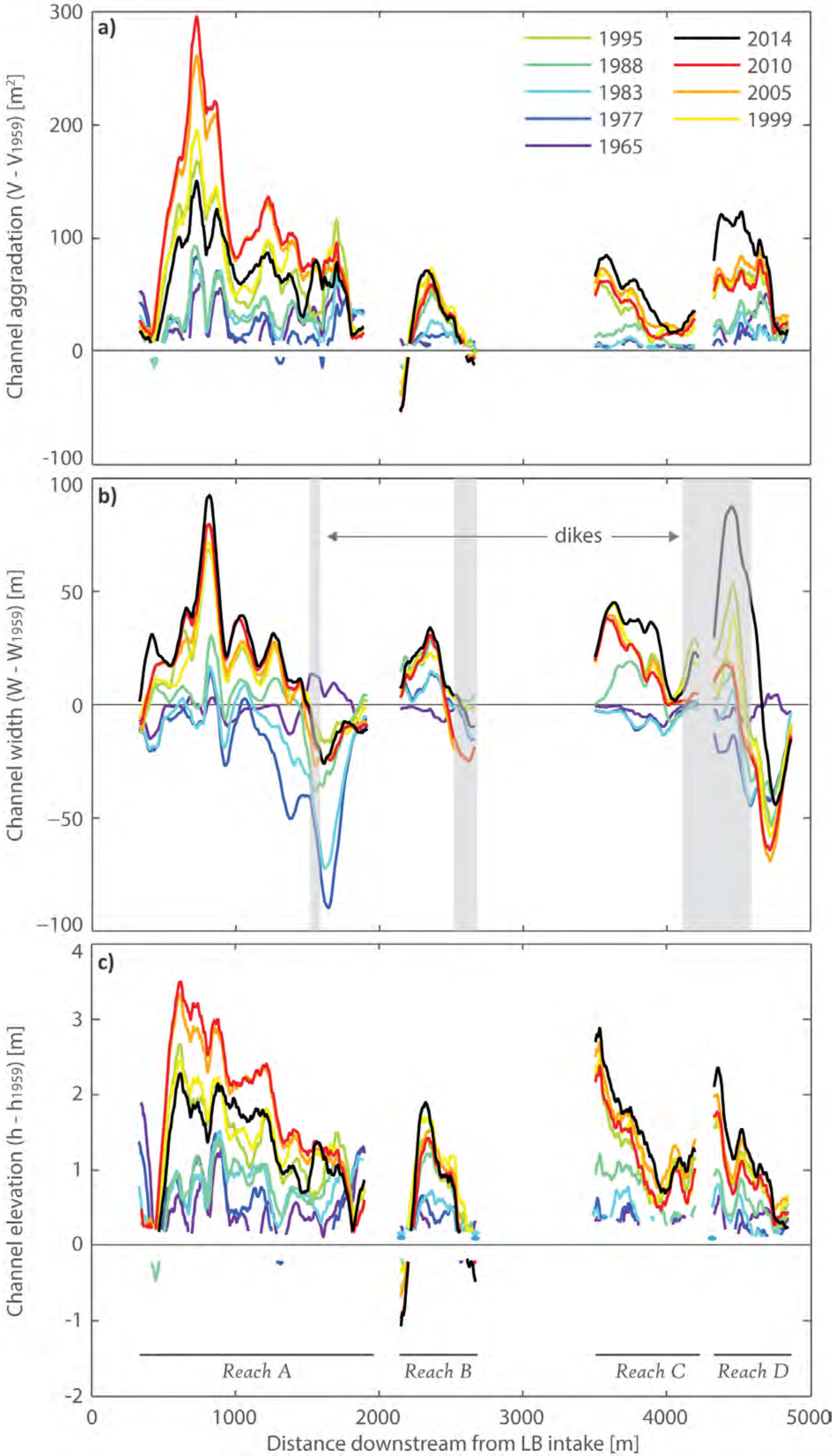

a)
b)
c)
1995
1988
1983
1977
1965
2014
2010
2005
1999
Channel aggradation (V - V1959) [m²]
Channel width (W - W1959) [m]
Channel elevation (h - h1959) [m]
dikes
Reach A
Reach B
Reach C
Reach D
Distance downstream from LB intake [m]
300
200
100
0
-100
50
−50
−100
4
3
2
1
-1
-2
1000
2000
3000
4000
5000

Figure 9.

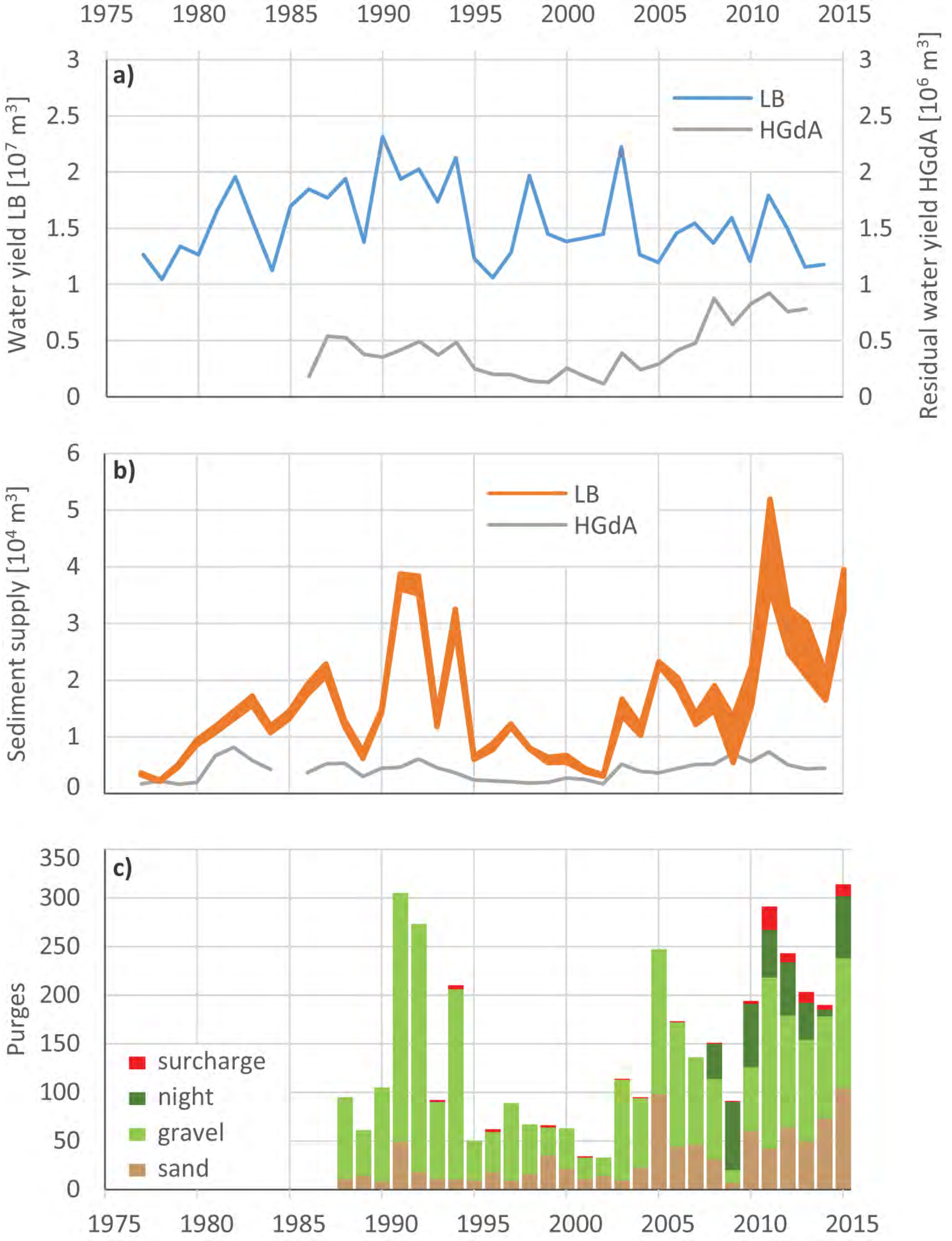

a)
LB
HGdA
Water yield LB [10^7 m^3]
Residual water yield HGdA [10^6 m^3]
b)
LB
HGdA
Sediment supply [10^4 m^3]
c)
Purges
surcharge
night
gravel
sand
1975
1980
1985
1990
1995
2000
2005
2010
2015

Figure 10.

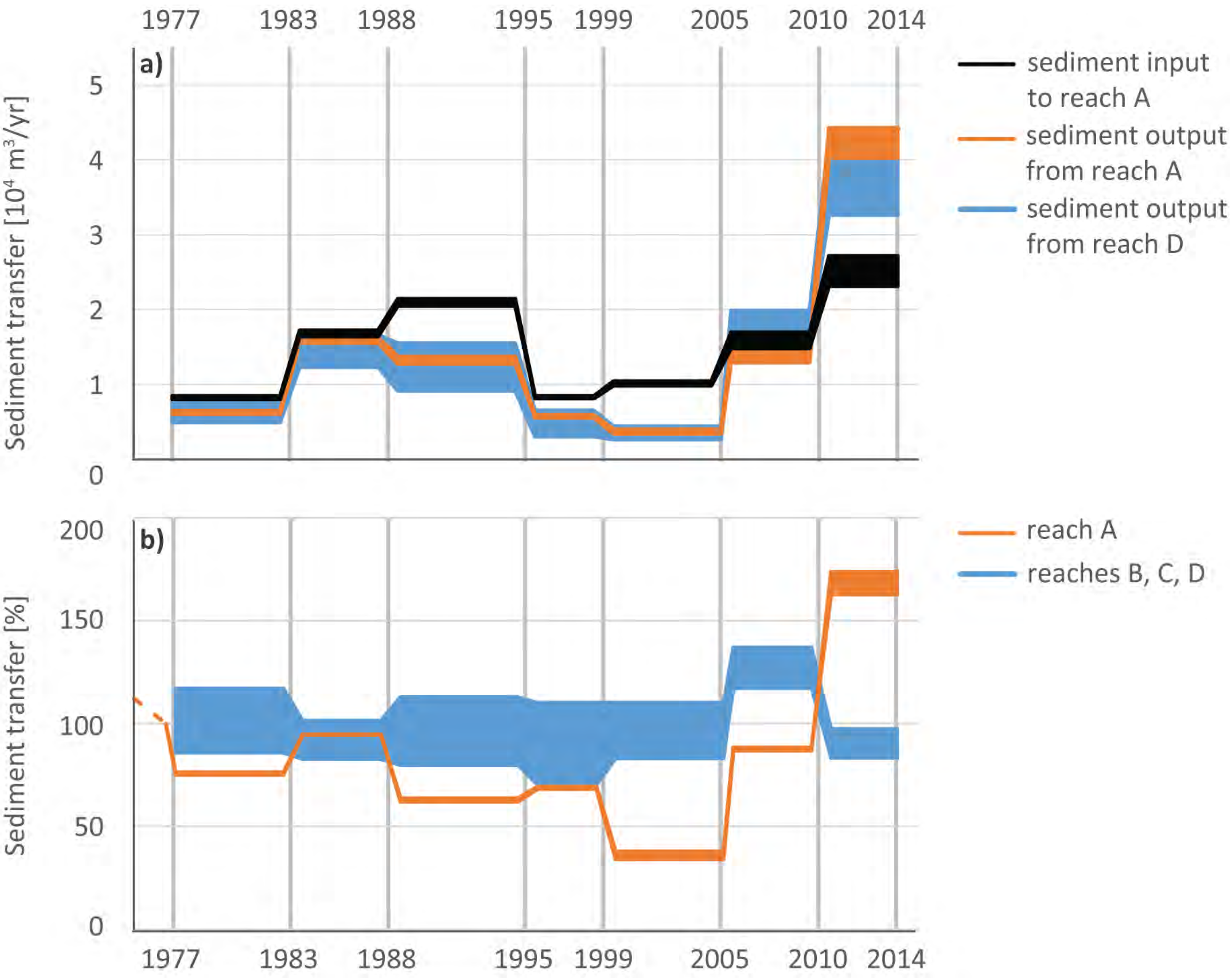
a)
b)
sediment input to reach A
sediment output from reach A
sediment output from reach D
reach A
reaches B, C, D
Sediment transfer [10⁴ m³/yr]
Sediment transfer [%]
1977
1983
1988
1995
1999
2005
2010
2014
0
1
2
3
4
5
50
100
150
200

Figure 11.

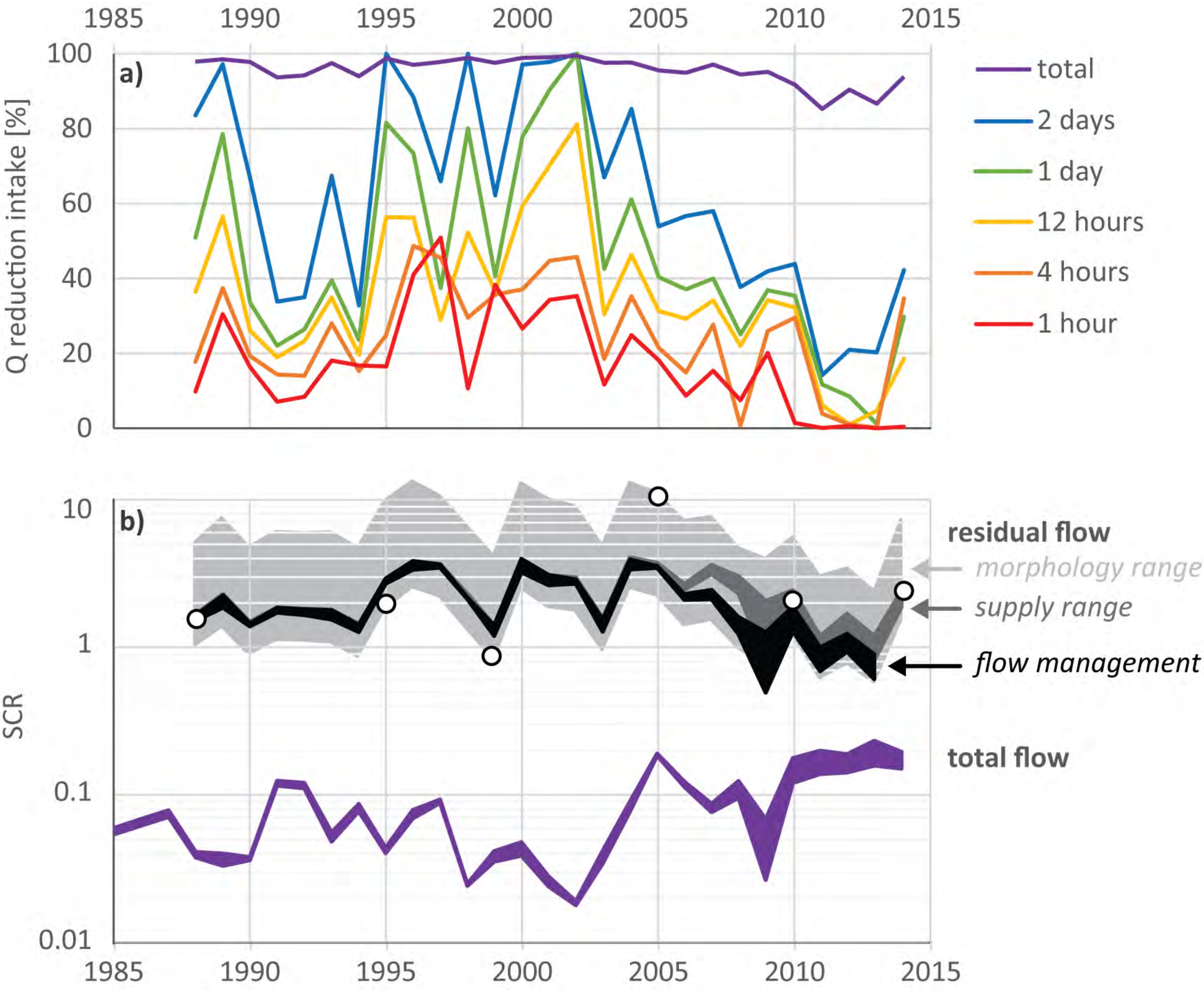

a)
Q reduction intake [%]
total
2 days
1 day
12 hours
4 hours
1 hour
b)
SCR
residual flow
morphology range
supply range
flow management
total flow
1985
1990
1995
2000
2005
2010
2015

Figure 12.

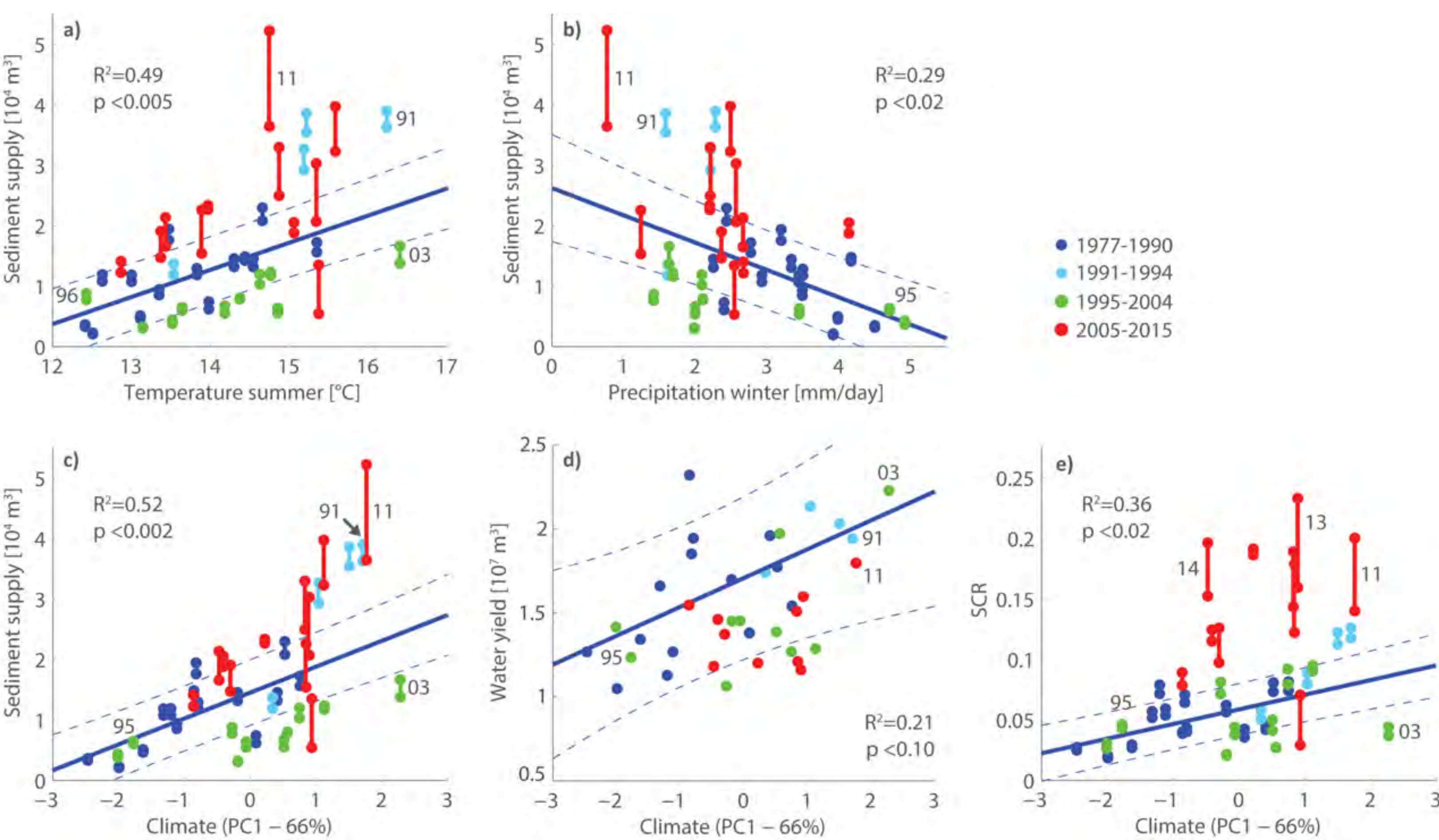

a)
R²=0.49
p <0.005
11
91
96
03
Sediment supply [10⁴ m³]
Temperature summer [°C]
b)
R²=0.29
p <0.02
11
91
95
Sediment supply [10⁴ m³]
Precipitation winter [mm/day]
1977-1990
1991-1994
1995-2004
2005-2015
c)
R²=0.52
p <0.002
91
11
95
03
Sediment supply [10⁴ m³]
Climate (PC1 – 66%)
d)
03
91
11
95
R²=0.21
p <0.10
Water yield [10⁷ m³]
Climate (PC1 – 66%)
e)
R²=0.36
p <0.02
13
14
11
95
03
SCR
Climate (PC1 – 66%)